CHAPTER 3

SYSTEMATIC EVALUATION OF THE COMBINATORIAL ACTIVITY OF BIOACTIVE MOLECULES FOR ISLET NEOGENESIS OF HUMAN BMSCS INTO FUNCTIONAL ISLETS

3.1. Introduction

Recently, cell therapy using autologous adult stem cells has been recognized for its potential to develop the field of regenerative medicine. Current progress in the field of regenerative therapies is concentrated on the differentiation of the pancreatic islet from various sources of stem cells. Numerous studies in the last decade have demonstrated the possibility of generating pancreatic islet /insulin-producing cells from various stem cell sources including embryonic stem cells (Mfopou *et al.* 2010, Shi 2010, Bose and Sudheer 2015), Induce pluripotent stem cells (Millman and Pagliuca 2017), and Adult MSC (Zanini *et al.* 2011, Marappagounder *et al.* 2013, Mitutsova *et al.* 2017). The potential of mouse adipose-derived stem cells to differentiate into ILCCs which bring euglycemia upon transplantation into STZ induced diabetes has been explored (Chandra *et al.* 2009). Dental pulp stromal /stem cells (DPSCs) could be differentiated into pancreatic endocrine progenitor lineage and offer an alternative and undisputable source of adult stem cells (Govindasamy *et al.* 2011). In similar studies, human DPSCs are differentiated into ILCCs and transplanted into STZ induced diabetic mice which restores normoglycemia (Kanafi *et al.* 2013). Comparison of differentiation of MSC obtained from human BM and adipose tissue into ILCCs *in vitro* concluded that hBMSCs are excellent to those from adipose tissue in the context of differentiation into ILCCs (Marappagounder *et al.* 2013). Furthermore, they also revealed the *in vitro* differentiation potential of human omentum fat-derived mesenchymal stem cells into ILCCs (Dhanasekaran *et al.* 2012). Pancreatic islet differentiation from various stem cell sources has been discussed earlier in the introduction of chapter number:1(see details in section number:1.14).

Moreover, reports suggest that mouse BMSCs are capable of *in vitro* trans-differentiation into functional pancreatic insulin-producing cells (IPCs) (Oh *et al.* 2004, Tang *et al.* 2004). Similar experiments with hBMSCs exhibited that they can differentiate into ILCCs *in vitro* by a mechanism link with various important transcription factors of the pancreatic islet developmental pathway when cultured in a designated culture condition (Moriscot *et al.* 2005). The hBMSCs isolated from adult diabetic patients have the potential to differentiate into ILCCs *in-vitro* (Sun *et al.* 2007). Hisanaga *et.al.*, 2008 developed a simple protocol to induced differentiation of mouse BMSCs to ILCCs using key bioactive molecules such as conophylline and betacellulin-delta4 (Hisanaga *et al.* 2008). The therapeutic consequence of transplantation of ILCCs -derived from hBMSCs confirmed that they were capable to manage STZ-induced diabetes in nude mice (Gabr *et al.* 2013). The recently same group showed a comparison of

three islet differentiation protocols in order to generate functional ILCCs from hBMSCs (Gabr *et al.* 2014). hBMSCs differentiate into endocrine pancreatic progenitor lineage *in-vivo* (Phadnis et al. 2011). Although there are some conflicting views about the trans-differentiation capacity of hBMSCs (Choi *et al.* 2003, Lechner *et al.* 2004, Røsland *et al.* 2009), bone marrow-derived mesenchymal stem cells are considered the most clinically accepted source for cell therapy for diabetes mellitus. Hence, all these experimental data support the potential of hBMSCs to differentiate into ILCCs. This can be achieved by stimulating molecular machinery using appropriate culture conditions along with differentiating molecules. However, the numerous stem cells require a different culture media condition and molecules to be differentiated into functional ILCCs, there are several molecules that can be used for islet differentiation e.g. activin A, exendin-4, KGF, betacellulin, nicotinamide, conophylline, etc. (Wong 2011).

Although from the review of literature it is evident that the *in vitro* differentiation of ILCCs from hBMSCs is a viable option, it still has a lot of room for improvement before they can be put to any clinical practice (Sun *et al.* 2007, Zanini *et al.* 2011, Pokrywczynska *et al.* 2015). Several factors can be thought of playing role in affecting the quality of islets obtained *in vitro*, some of them are enlisted below: (1) Lack of participation of the seeded hBMSCs ultimately reduces the number of cells undergoing differentiation thus decreasing islet yield and functionality (Zanini *et al.* 2011) (2) Optimization of culture condition such as air-liquid interface culture, 3D culture promoting surface modification for islet differentiation may support for preventing dedifferentiation and increasing islet functionality (Aloysious and Nair 2014, Li *et al.* 2016) (3) The Need for better differentiating agents may help in improving the islet quality relative to previously used differentiating agents like conophylline, exendin-4, activin-A, glucagon-like peptide-1, nicotinamide, etc.(Gabr *et al.* 2014).

Bioactive molecules/ compounds are defined as small quantities in various diets such as fruits, vegetables and whole grains that support human health and capable of positively modulating metabolic and physiological cellular processes in humans that consume them (Oh and Jun 2014). Several bioactive molecules are identified in vegetables and fruits that work as anti-inflammatories, anti-oxidants, inhibition or induction of enzymes /receptors and protective against metabolic disorders like diabetes and heart disease (Santos *et al.* 2019). Plant-derived bioactive molecules are utilized extensively as an anti-diabetic drug of choice because of their high efficacy, less adverse effect, and inexpensive (Grover and Vats 2001). Currently, much

consideration has been given to nutraceutical components (bioactive molecules) that might be valuable for the prevention of metabolic disease like diabetes, as various research groups have shown beneficial effects of bioactive molecules on pancreatic islets survival, antioxidant activity, and reduction in central necrosis, and so forth (Oh and Jun 2014). The majority of these compounds are derived from plant sources and figure 1.13 depicts several bioactive compounds derived from different plant sources and animal source.

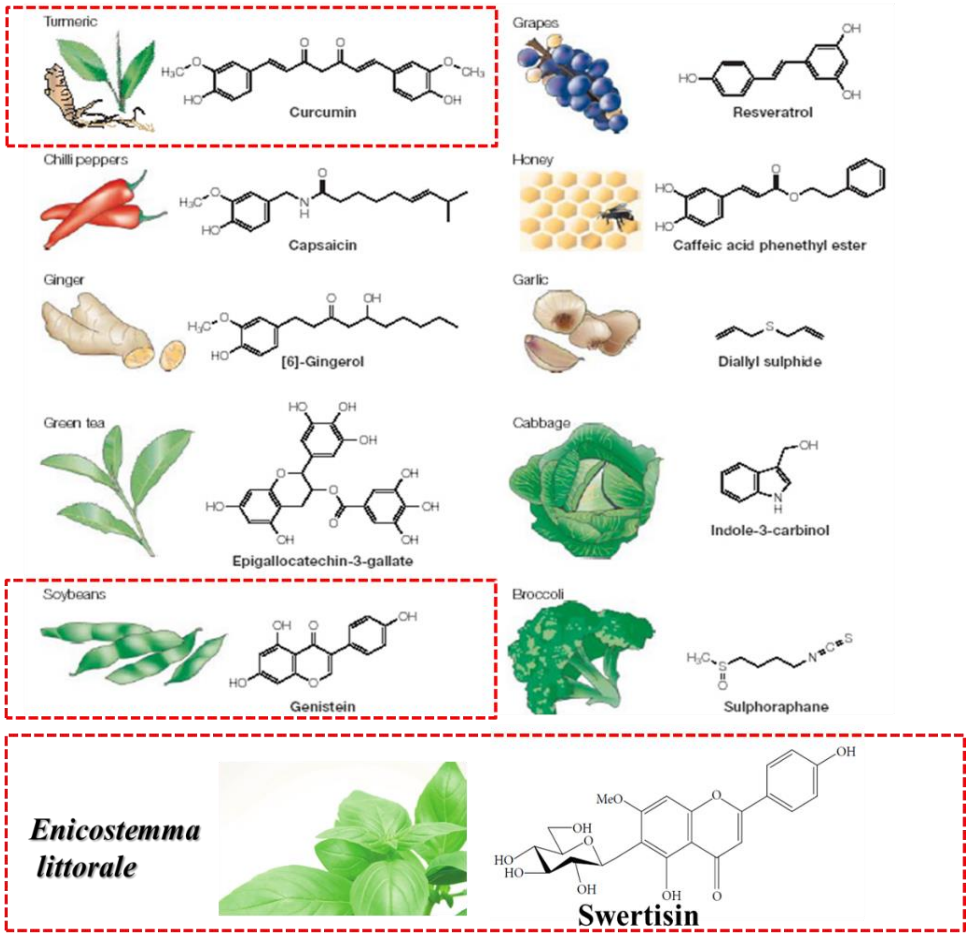

Figure 3. 1 Structural feature of herbal medicinal plants (animal product: honey) and its bioactive molecules (active ingredients) that affect pancreatic islets function and diabetes.

In the current study, we have employed swertisin, an isolated bioactive from *Enicostemma littorale (*EL). Earlier reports from our lab demonstrated potentials of swertisin for *in-vitro* islet differentiation and improved glucose homeostasis when transplanted in diabetic animals *in vivo* (Gupta S *et al.* 2010, Dadheech *et al.* 2013). we also elucidated its molecular mechanism in islet neogenesis (Dadheech *et al.* 2015). Very recently, we also demonstrated that PREPs (Pancreatic resident endocrine progenitors) rapidly differentiated into mature ILCCs by

swertisin molecules (Srivastava *et al.* 2019). Further, we also explored the role of swertisin in prompting mouse pancreatic resident progenitors for islet differentiation in an STZ induced diabetic mouse model (Srivastava *et al.* 2018).

Here, we have tried to emphasize that a small bioactive molecule i.e. swertisin and other bio-molecules i.e. curcumin (Kanitkar and Bhonde 2008, Kanitkar *et al.* 2008, Zhang *et al.* 2013), genistein (Jonas *et al.* 1995, Liu *et al.* 2006, Gilbert and Liu 2013) along with human BMSCs with their islet differentiation capability can provide a spectacular therapeutic intervention for autologous stem transplantation in DM patients. We expect these optimized islets differentiation protocol to be more effective in terms of functionality and longevity for providing better treatment and extended relief from successive insulin oral administration and optimized islets can be translated for the human clinical trial purpose for treating diabetes mellitus.

To fully realize the potential of hBMSCs and bioactive molecules cocktail (BMC), various fundamental questions need to be addressed. (1) Can bioactive molecules cocktail trigger hBMSCs islet differentiation from hBMSCs into ILCCs? (2) Whether culture condition modification like ultra-low adherence (ULA) plates, enhanced differentiated ILCCs yields? (4) Do bioactive molecules have any role in reinforcing differentiated ILCCs viability? (5) Does differentiated ILCCs release c-peptide in response to *in vitro* glucose stimulation?

To address these questions and expand our knowledge on the pancreatic islet differentiation. Thus, we segregated our major objective into three sub-objectives:

(a) Isolation and characterization of hBMSCs
(b) Islet differentiation from hBMSCs into ILCCs using bioactive molecule cocktail
(c) Functional characterization of differentiated ILCCs

3.2. Experimental design

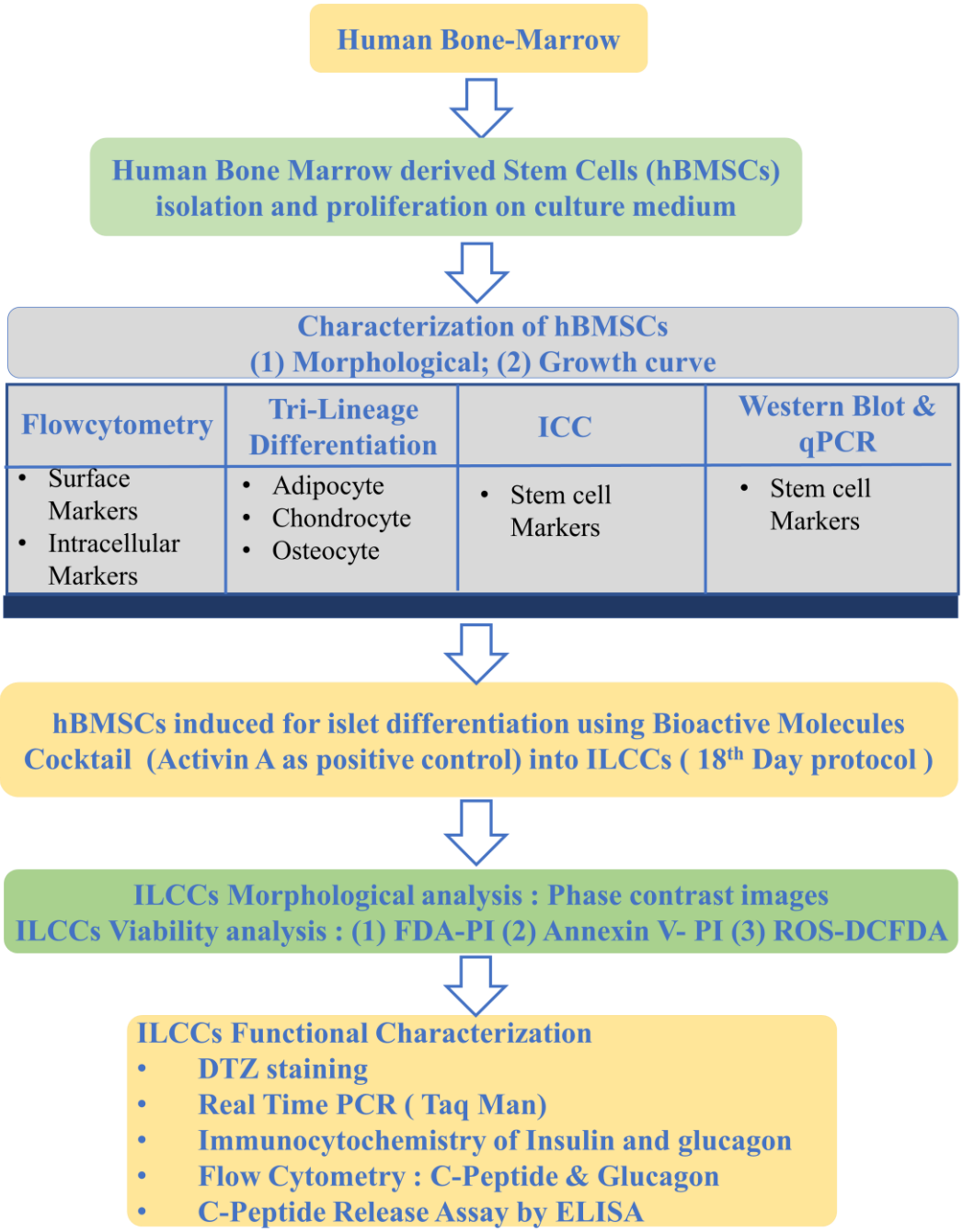

Figure 3. 2: Representative flowchart of experimental design of chapter:3

3.3. Material and method

3.3.1. Materials

All chemicals and culture media used in this study were purchased from Gibco, Sigma Aldrich, Thermo Fisher Scientific. The details of the primary and secondary antibodies used are given in annexure -II. Molecular biological reagents, cDNA synthesis kit, and qPCR kit were procured from ABI (Thermo scientific, USA). All cell culture related plasticware were purchased from Nunc^{TM} Inc., (Thermo scientific, USA), and Eppendorf (Germany).

3.3.2. Methods:

A. Isolation and characterization of hBMSCs

All samples were collected by an orthopaedic surgeon after patients (Human Subject) were informed about the experimental study and signed an informed consent form. The protocol has been approved by the Institutional Review Board of The M.S. University of Baroda (Human Ethical clearance number: FS/IECHR/2014/4). Under aseptic conditions, 5-8 ml of heparinized BM samples were collected from the tibia/femur of six healthy human subjects (N=6) 18-55 years of age (Table: 3.1).

Sr.	Bone Marrow aspiration location	Donor Sex (M/F)	Donor Age	Disease Status
1	Tibia	M	17	Normal(Healthy)
2	Tibia(Interlock)	F	45	Normal(Healthy)
3	Tibia	M	35	Normal(Healthy)
4	Femur	M	22	Normal(Healthy)
5	Tibia(Interlock)	M	24	Normal(Healthy)
6	Femur	M	48	Normal(Healthy)

Human Subject Selection Criteria	Inclusion Criteria	Exclusion Criteria
Age (Year)	10-60	Above 60
Disease status	Normal Healthy, Diabetes (Type-I, Type-II)	Any Bone Marrow related diseases, Any types of Cancer, Any Genetic diseases, Metabolic disorder other than diabetes.

Table 3. 1: Characterization of human bone marrow volunteers and including & excluding criteria for human subject was enrolled in human bone marrow-derived mesenchymal stem cells isolation study.

Bone marrow samples were transferred into sterile heparinized collection tubes, then isolated and cultured hBMSCs as described in Jafarian et al.,2014 (Jafarian *et al.* 2014) . Briefly, whole BM was diluted with incomplete low glucose Dulbecco's modified Eagle's medium (DMEM-LG,5.56 mmol/L, Sigma-Aldrich, USA) media after which mononuclear cells were isolated using HiSep LSM1077(1.077 + 0.0010 g/ml, Hi-Media, India). After centrifugation for 30 min. at 400 x g, mononuclear cells were removed from plasma/HiSep LSM1077 interface, and cultured in 5 ml of DMEM LG supplemented with 10 % FBS (Gibco, South America origin, USA), 100 U/ml penicillin and 100 U/ml streptomycin (Pentrep, Gibco, USA). After standard nucleated cell counting, mononuclear cells were seeded at a density of 5 x 10^6 per 25-cm^2 and then incubated at 37 ºC in 5 % humidified CO_2. After 72 hrs., the non-adherent cells were removed and adherent cells were cultured for approximately 2-3 weeks. The fresh complete medium was replaced twice per week. Primary cultures were maintained for 15-20 days. Upon reaching approximately 90-95 % confluency, cells were collected with a solution of 0.25 % trypsin (Sigma-Aldrich, USA) and 1 mM EDTA (Sigma-Aldrich, USA) for 2-5 min at 37 ºC. After centrifugation, cells were re-plated in a 75 cm^2 flask to achieve the required confluency and referred to as the first-passage culture. Further, hBMSCs (Passage # 3-6) were cultured in DMEM Knock out (DMEM-KO, Gibco, USA) containing 10 % FBS.

B. Cell count and growth curve:

Approximately 80 %- 90 % confluent hBMSCs (P# 3-6) were trypsinized with 0.1 % trypsin EDTA solution and calculated under a phase-contrast microscope (Eclipse TE 2000 inverted microscope, Nikon, Japan) on Neubauer chamber using 0.05% trypan blue dye. Twenty thousand hBMSCs (P#3-6) were seeded into each well of 24 well plates for growth curve analysis. hBMSCs were eventually trypsinized and calculated at different time points (0day,1 day,2day,3day, 4day, 5day, 6day, and 7day). A graph of growth curve was plotted against time (days)/ number of hBMSCs.

C. Flow cytometric analysis of surface marker and intracellular marker staining

i. Surface marker

hBMSCs were trypsinized and resuspended 0.5 million cells per tube in 100 µl of staining media (PBS containing 1 % BSA). The required primary antibody as per antibody company manufacturer's recommended (Refer appendix (B) for specifications of antibody) was Incubated with hBMSCs for 30 min. in a dark place at 4º C. hBMSCs washed two times with staining media and pelleted down by centrifuge at 600 g for 5 min. at 4º C. hBMSCs were

suspended in 250 µl staining media and analyzed on flow cytometry (BD FACS ARIA III, BD bioscience, USA) by collecting 10,000 events, as described in our previous report Srivastava et al., 2018. FlowJo software (Becton *Dickinson, OR*, USA) was employed for the analysis of flow cytometry data.

ii. Intracellular marker

hBMSCs were trypsinized and resuspend 0.5 million cells per tube in 100 µl of staining media. hBMSCs were fixed with 2 % PFA for 10 min at 25º C. hBMSCs were washed twice with staining media. After centrifuging at 600 g for 5 min at 4º C, resuspend pellet with 450 µl ice-cold analytical grade methanol per 0.5 million cells, incubated 4º C for 10 min. hBMSCs washed twice with staining media. The required primary monoclonal antibody (1ºAb) as per antibody company manufacturers recommended in each tube was supplemented. hBMSCs were incubated with primary antibody for 30 min at 4º C. In the case of the primary antibody was not fluorescently labelled, the samples were additionally stained with its respective fluorescent-labelled secondary antibody (2ºAb) for 30 min at 25º C in dark. (Refer appendix: B for specifications of antibody). Further, hBMSCs were suspended in 250 µl staining media and analyzed on flow cytometry (BD FACS ARIA III, BD bioscience, USA) by collecting 10,000 events, as described in our previous report Srivastava *et al.*, 2019 (Srivastava *et al.* 2019). FlowJo software (Becton *Dickinson, OR*, USA) was employed for the analysis of flow cytometry data.

D. Immunocytochemistry

hBMSCs and differentiated islets-like clusters were cultured, harvested, and fixed with 4% paraformaldehyde for 10 min. at room temperature on a coverslip. Cells and clusters were washed with 1X PBS followed by permeabilized with 0.01% Triton X-100 for 2-4 min. on ice. Again, the washing step was performed, incubated in a blocking buffer containing 0.5% BSA+0.1% FBS in PBS for 1 hour at room temperature. Samples were treated with primary antibodies at 4°C overnight. Samples were washed with 1XPBS post-incubation followed by secondary antibody incubation (in case of unlabelled primary antibodies) for 1 hour at room temperature (Antibody details in appendix: C). Samples were again washed and counterstained with DAPI and mounted on glass slides in mounting media. The fluorescence images were captured using confocal microscopes (Zeiss/Nikon/Olympus).

E. Western blot analysis

hBMSCs and islet-like cell clusters (ILCCs) were harvested at specific periods as discussed in the plan of work. Briefly, samples were washed in chilled 1X PBS, centrifuged, and resuspended in Laemmli buffer (SDS, Tris-ClpH-7.4, Urea, β-Mercaptoethanol, EDTA, Bromophenol Blue). Harvested samples were then subjected to sonication at 45% amplitude for 20 secs with 2 sec/0.2 sec on/off the pulse. Total protein concentration was estimated by Bradford's method and 20µg of total protein was resolved on 12% SDS-PAGE gels at 100V. Proteins were then transferred on nitrocellulose membrane at 100V for 1:30 hours and confirmed transfer with Ponceau S stain. The blot was then subjected to the elimination of non-specific binding by blocking buffer (5% Skimmed milk solids; 0.1% Tween 20; 1XPBS) for 1 hour at room temperature. Primary antibodies against specific proteins (as mentioned in appendix :D) were incubated overnight at 4°C, with gentle agitation, followed by washing with 1XPBS+0.1% Tween20 (4×15 min.), incubation with specific HRP labelled secondary antibodies for 1 hour at room temperature with gentle agitation and again by washing with 1XPBS+0.1% Tween 20 (4×15 min.) and with 1X PBS (2×15 min). Specific protein bands were developed using enhanced chemiluminescence (ECL) reagent (Bio-Rad) and visualized in chemidoc (UV tech, Alliance Model 4.7, Cambridge). Protein band density was determined by ImageJ software (NIH, USA) and normalized with β-ACTIN/GAPDH served as a loading control.

F. Gene expression study

Samples (hBMSCs & ILCCs) were harvested by centrifugation and resuspension in Trizol (Invitrogen, USA) reagent followed by isolation of total RNA as per manufacturer's protocol. Total RNA was quantified on UV Spectrophotometer (Cary 60 UV-Vis Spectrophotometer, Agilent technology, USA) and mRNA to cDNA conversion was carried out using high-capacity cDNA synthesis kit (ABI, USA) as per the kit instructions on gradient PCR (T-100 Thermal cycle, Bio-Rad, USA). Expression of targeted genes was determined via qPCR technique using SYBR green chemistry (7500 Applied Biosystem Real-Time PCR, USA) or TaqMan chemistry (12k flask Quant Studio Applied Biosystem, USA) using specific primers (Appendix: A). Ct values of Actβ served as an internal control for gene expression Ct values to calculate ΔCt. The ΔΔCt of the gene was determined from the ΔCt of test group-ΔCt of the control group and relative fold change [$2^{-(\Delta\Delta Ct)}$] of gene expression was plotted on a graph.

G. Differentiation of hBMSCs into adipocytes, osteocytes, chondrocyte (Trilineage Differentiation)

hBMSCs at passages 3-6 were utilized for differentiation into adipocytes, osteocytes, and chondrocytes. The hBMSCs were seeded at 10^5 cells /well into a six-well plate. When the cells reached 85-95 % confluency, they were incubated in adipogenic, osteogenic, chondrogenic medium for 18,20, and 21 days respectively. Adipogenesis was induced by treatment of 10 mM dexamethasone (Sigma, USA), 0.5 mM 3-isobutyl 1-methylxanthine (IBMX), 200 µM indomethacin, 0.5 µg/ml insulin in DMEM Low Glucose with 10 % FBS for 18 Day. The culture media was replaced every alternative day. On Day 18, the cells were washed with PBS, fixed with 4 % paraformaldehyde (PFA) for 10 min, rinsed with PBS and exposed to oil-red-O (Sigma, USA) and observed under an inverted phase-contrast microscope. For osteogenic differentiation, the cells were cultured for 20 days in an osteogenic medium that contains DMEM low glucose with 10% FBS, 0.1µM dexamethasone, 10mM β-glycerophosphate, 2mM ascorbic acid. After 20 days, the cells were fixed in 4% PFA for 15 min, washed with PBS, and stained with alizarin red stain (Sigma) for 10 min and observed in a phase-contrast microscope. For chondrogenic differentiation, the cells were cultured for 21 days in a chondrogenic medium that contains DMEM low glucose with 10 % FBS, 10mM Dexamethasone, and 10 mg/L insulin. After 21 days, cells were fixed with 4 % PFA for 15 min, washed with PBS, and stained with 1% Alcian blue for 15min and observed in the phase-contrast microscope.

H. Islets Differentiation protocol

Initially, hBMSCs were differentiated into ILCCs with 10^{th} day islet differentiation protocol as described in our lab study with mouse BMSCs as stem cells source and swertisin as a bioactive molecule. Later we shifted to 18^{th} day islet differentiation protocol with some major modification to our previous protocol and eventually, we developed novel islet differentiation protocol and filed in Indian patent (application number:201621012988). Briefly, hBMSCs between passage number 3-6 (70–80 % confluent) were trypsinized. hBMSCs were centrifuged at 1000 rpm for 10 min. and the pellet was washed with 1x PBS to remove the residual serum-containing medium. hBMSCs were suspended in the differentiation medium (0.25 million cells/ml) and were seeded in the ultralow adherence six-well plates (Corning, USA) [Initially, we used non-tissue culture treated six-well plates] with 2ml of the differentiation medium. Our pancreatic islet differentiation protocol was divided into four multi-stages. In the first stage (0-5 day), the hBMSCs were cultured for 5 days in serum-free medium, DMEM high glucose

(Sigma, USA), 1 % BSA (SRL, India), 10 ng/ml activin A (Sigma, USA) or 15µg/ml swertisin (as test group) as previously described (Dadheech *et al.* 2013, Dadheech *et al.* 2015, Srivastava *et al.* 2019), 1 mM sodium Butyrate (Sigma, USA), 1µM retinoic acid (Sigma, USA), 100pM HGF (Gibco, Thermo scientific, USA). In second stage (5-10day) media replaced with 10µg/ml FGF (Gibco, Thermo scientific, USA), 20 µg/ml EGF (Gibco, Thermo scientific, USA),15µg/ml swertisin or 10ng/ml activin A. In the third stage (10-15 day), the cell cluster aggregate was switched to media that contained DMEM low Glucose with 1 % BSA, 10 nM exendin-4 (Sigma, USA), 10 mM nicotinamide (Sigma), 15µg/ml swertisin or 10ng/ml activin A. In the last stage (15-18 day), media replaced with 100nM Exedin-4, N2 and B27 supplement's (Gibco, Thermo scientific, USA),10ng/ml activin A or bioactive molecules cocktail (BMC) [15µg swertisin + 10µM curcumin (Sigma, USA) (Meghana *et al.* 2007) + 5µM Genistein (Sigma, USA) (Gilbert and Liu 2013). Differentiated ILCCs were washed three times with PBS and observed in a phase-contrast microscope (Nikon, Japan) and photographed. Morphometry analysis of ILCCs was performed using NIS-Element imaging software (Nikon, Japan)

I. DTZ staining protocol

DTZ staining protocol was performed as described in (Komatsu *et al.* 2016). In brief, pellet down 10^{th} and 18^{th} day ILCCs in 1.5 ml tube & incubate at 37ºC for 15-30 min by adding DTZ working solution (Sigma, USA). Wash the pellet twice with PBS to remove excess DTZ stain. Observed under an inverted phase-contrast microscope (Eclipse TE 2000 inverted microscope, Nikon, Japan).

J. MTT assay

hBMSCs were plated in cell culture treated 96-well plate for respective curcumin treatments (Curcumin concentration 2µM, 4µM, 5µM, 6µM, 8µM, 10µM, 12µM, 15µM, 20µM, 50 µM,100 µM). After the 48 hours pre-treatment period, 10 µl of 5 mg/ml MTT (Sigma-Aldrich, USA) solution was added per 90 µl of the media followed by incubation for 3 hours at room temperature in a dark place. After incubation, MTT containing culture media was gently removed by media aspirator unit, 100 µl DMSO was added, mixed well, and incubated for 30 min at room temperature in a dark place. These plates were then read at 570 nm in a microplate reader (Multiskan EX, Thermo Scientific, USA).

K. FDA-PI staining

FDA-PI dual staining was performed to make a distinction between the live and death population by confocal microscope as described in our paper (Srivastava *et al.* 2016) using FDA and PI dye (Sigma Aldrich, USA). Briefly, collect 18th day ILCCs in a tube by centrifuge at 300 g for 5 min at 25º C. Addition of FDA (5mg/ml) and PI (2 mg/ml) staining solution in ILCCS pellet and incubate samples at 25 ºC for 5-10 min in dark. Remove excess staining by washed with PBS. After clusters transferred into the optical clear bottom 6 well plate and analyzed samples using confocal laser scanning microscope (FV3000, Olympus, USA).

L. Annexin V-PI staining protocol for apoptosis assay

Annexin V-PI dual staining was performed to make a distinction between apoptotic and necrotic cell death population by flow cytometry as described in kit manufacture instruction (FITC Annexin V apoptosis detection kit, BD Pharmingen, USA). Briefly, centrifuge 18th day ILCCs at 300 g for 2 min at 25ºC. Remove supernatant and ILCCS pellet resuspend in a trypsin-EDTA solution for 10 min at 37º C to prepare a single cell from ILCCs. Dissociate the ILCCs by pipetting up and down 15-20 times using a 1 ml pipet tip until no visible clusters are left. Add 10 ml serum-containing culture medium into a tube to terminate the trypsin EDTA reaction and pass the dissociated cell suspension through a 70 µm pore size filter (Cell Stainer) to remove larger clumps (Undigested ILCCs), then centrifuge for 5 min at 300g. Single cells were washed with PBS and resuspended in 1 X binding buffer, further staining protocol was followed as described in kit manufacture instruction (FITC Annexin V apoptosis detection kit, BD Pharmingen, USA). Finally, the single cells were resuspended in 200 µl staining media (PBS+1%BSA) and as soon as possible (within 1 hrs.), analyze the stained single cells by flow cytometry. Further, flow cytometry data were analyzed using FlowJo software (Becton Dickinson, OR, USA).

M. Intracellular reactive oxygen species (ROS) detection assay

Intracellular reactive oxygen species (ROS) level (DCFH-DA: Fluorescent) can be detected by two methods (a) titration in a multimode reader (Synergy™ HTX Multi-Mode Microplate Reader, BioTek, USA) (b) inverted fluorescence microscopy (Eclipse TE 2000 inverted microscope, Nikon, Japan).

i. Multimode reader:

Cultivate differentiated ILCCs in an under standard culture condition. Harvest an equal number of ILCCs per sample/ group into a 0.5 mL tube (Handpick differentiated ILCCs). Wash ILCCs by centrifugation (500 g) for 5 min. using PBS. Repeat this step one more time and remove supernatant. Resuspend the ILCCs pellets in 20 µM of DCFH-DA solution (Sigma Aldrich, USA). Incubate ILCCs with DCFH-DA solution for 30 min at room temperature in the dark. Then, centrifuge ILCCs 500 g for 5 min and remove the supernatant containing the DCFH-DA solution. Resuspend ILCCs in 100µl per tube PBS and place them into black /clear bottom microtiter 96 well plates. Measure DCF fluorescence using a fluorescence microtiter plate reader (Ex:485 nm/Em:528 nm) [Synergy™ HTX Multi-Mode Microplate Reader, BioTek, USA]. Hoechst dye used for the normalization of nucleus content (Ex: 360nm/Em:460 nm). A graph of ROS level was plotted against fluorescence intensity against the sample.

ii. Inverted fluorescence microscopy:

The generated cellular ROS by DCFH-DA staining protocol was visualized by an inverted fluorescence microscope. To detect intracellular ROS accumulation, the ILCCs were plated in 12 well plates. Wash ILCCs twice with 1 X PBS. Stain cells with 20 µM DCFH-DA for 30 min. at 37º C in a dark place. After the incubation period, wash ILCCs twice with 1X PBS. DCFH-DA green fluorescence was observed using an inverted fluorescence microscope (Eclipse TE 2000 inverted microscope, Nikon, Japan). The relative ILCCs fluorescence intensity was calculated by Image J software (NIH, Bethesda, USA).

N. Human c-peptide release assay

For glucose-stimulated c-peptide release assay, on day 18, about 100 day-18 ILCCs were handpicked in the Eppendorf tube. ILCCs were then washed three times with PBS and incubated with freshly prepared KRBH buffer (Gerdes *et al.* 2014). ILCCs (from activin A & BMC) & undifferentiated hBMSCs (Control) were challenged 5 mM(Glucose), 25 mM(Glucose), 30mM KCI (Potassium chloride, SRL) in KRBH buffer, respectively, as discussed in our previous reports (Dadheech *et al.* 2013, Srivastava *et al.* 2019).The human c-peptide release was detected in chemiluminescence ELISA multimode reader (Synergy™ HTX Multi-Mode Microplate Reader, BioTek, USA) using STELLUX^{TM} human c-peptide chemiluminescence ELISA (ALPCO, USA) kit. ELISA standard protocol was carried out according to kit instructions.

O. Statistical analysis

Results are displayed as mean ± SEM of the demonstrated number of experiments. Statistical significance was performed using the unpaired student's t-test or two-way analysis of variance using Bonferroni post-test using graph pad prism software version 6. P-value < 0.05 was counted to be statistically significant.

3.4. Results

3.4.1. hBMSCs isolation from healthy human bone marrow

hBMSCs were isolated, cultured, and propagated from the bone marrow of six human subjects after informed consent. hBMSCs readily adhered and proliferated on tissue culture-grade plastic dish and were successfully proliferated until 3-6 passages. Phase micrographs of isolated hBMSCs (Figure:3.3) showed the distinct morphology of typical stromal cells with a spindle-shaped appearance. hBMSCs reached confluency within 8-10 days and exhibited a homogenous cell population by passage-2. The growth pattern of hBMSCs analyzed by direct cell count demonstrated that the lag phase of hBMSCs completed within 2 days, leading to 4 days of log phase (Figure:3.3). The hBMSCs cultures exhibited an increased rate of proliferation between passage 2-6 with a homogeneous fibroblastic morphology till 8-10 passages.

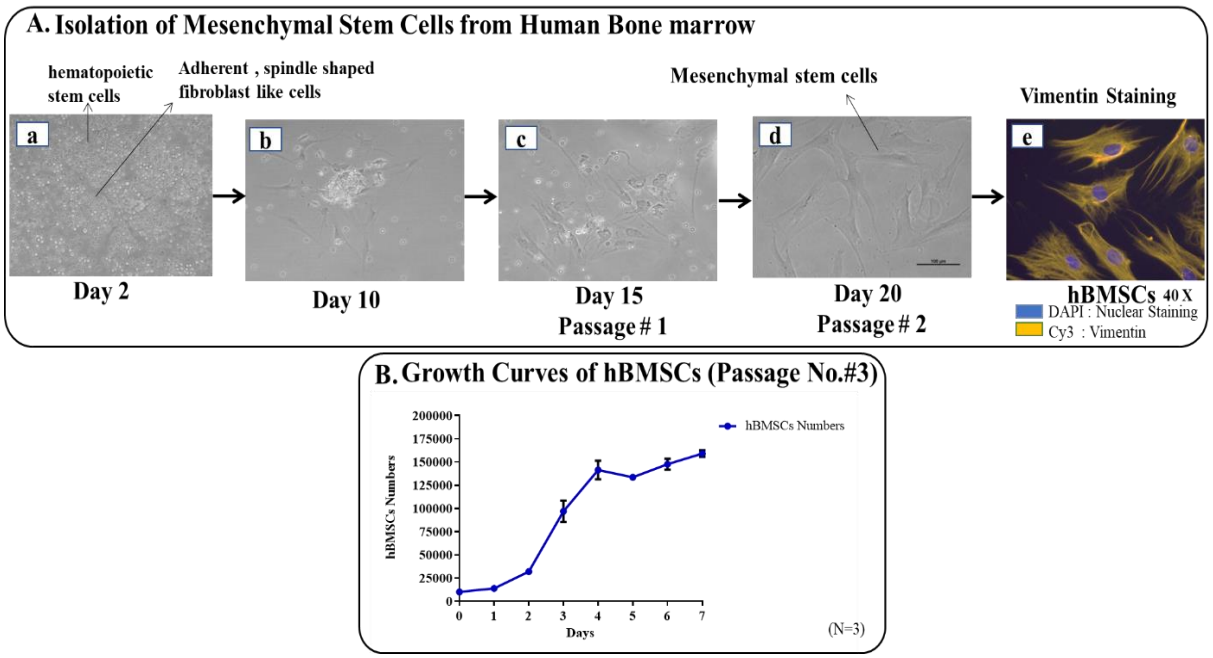

Figure 3. 3: Isolation and characterization of hBMSCs from Human BM subjects. (A) hBMSCs were isolated from adult human BM in KO-DMEM media. Phase-contrast microscopy plates

showed adherent, spindle-shaped fibroblast-like cells (image: a to d) after two days of seeding. hBMSCs proliferated in media reached 80-90 % confluent by day 15 (Passage #1) and approximately day 20 reached at passage # 2. The immunofluorescent micrography showed the cells stained positive for vimentin (Cy3 labeled: yellow color) -mesenchymal marker & the nucleus was stained with DAPI (blue color). Scale bar – 50 µm. (B) Growth curve patterns of hBMSCs at passage #3. hBMSCs showed the log phase between day 2 to day 4.

3.4.2. Characterization of patient-derived hBMSCs

A nominal immune positive criterion for the detection of hBMSCs cells is the presence of CD105, and CD44 while being negative for CD34, CD31. Hence purified hBMSCs from BM were characterized by these cell markers expressed on their surface by cytometry. At passage (P) 4, Flow cytometry analyses revealed that hBMSCs were strongly positive for MSC marker CD44 (99.9%) and CD105(83.6%) (Figure: 3.4) but were negative for hematopoietic marker CD34(0.21%) and CD31(0.48%) (Figure: 3.4). Moreover, flow cytometry result demonstrated that hBMSCs expressed Nestin (99.0%), STRO-1(77.9%), vimentin (99.7%), α-SMA (98.7%), fibronectin (61.1%) markers and Ki67 (75.6%) a proliferation marker (Figure :3.5). These markers were further evaluated by immunocytochemistry using confocal microscopy (Figure:3.5).

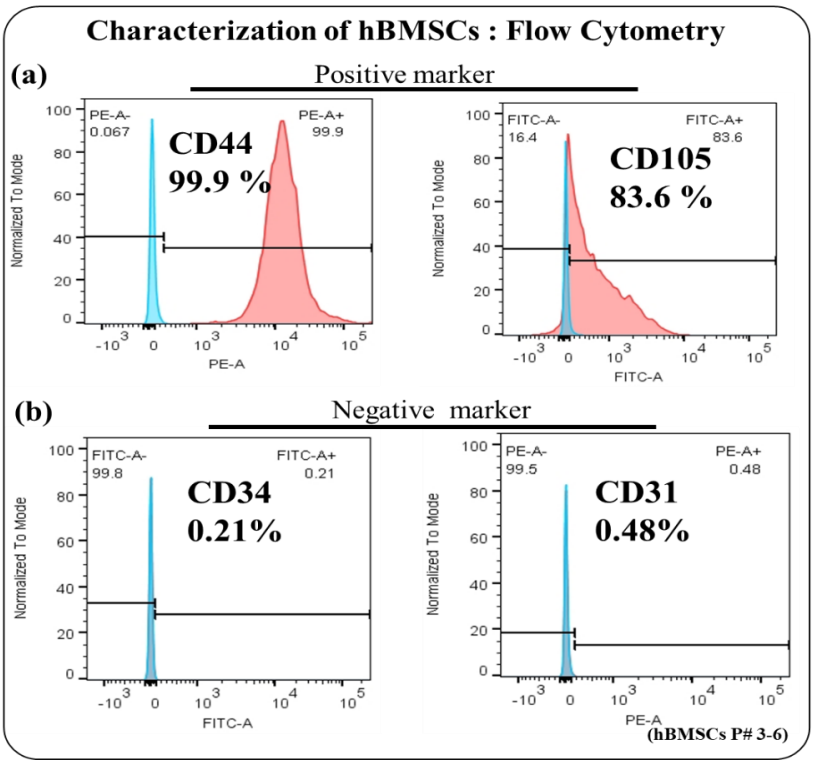

Figure 3. 4: Characterization of isolated hBMSCs (Human BM) using flow cytometry: (a) hBMSCs were positive for mesenchymal stem cells surface markers such as CD 44 and CD 105. (b) hBMSCs were negative for hematopoietic stem cells surface markers such as CD34 and CD 31 (N=3).

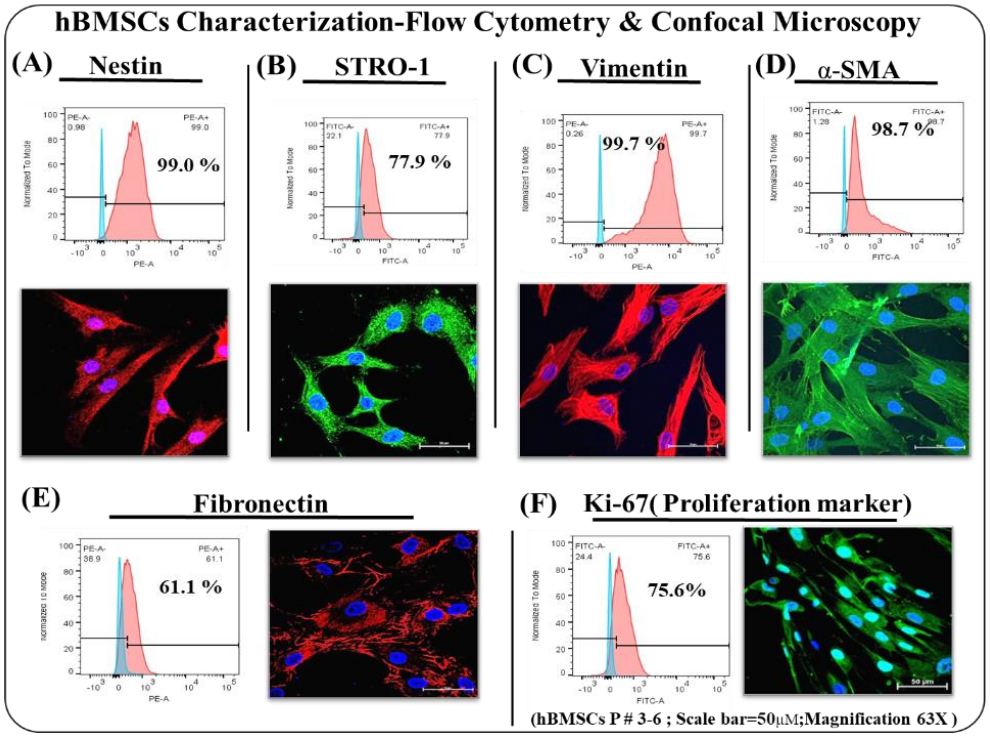

Figure 3. 5: Characterization of hBMSCs for stem cell and mesenchymal marker using both techniques confocal microscopy and flow cytometry: Immunocytochemistry was performed to identify nestin (Red), STRO-1(Green), vimentin (Red), α-smooth muscle actin (Green), Fibronectin (Red) and proliferation marker ki67 (Green). Counterstaining of nuclei was done by DAPI (as shown in Blue). Further, flow cytometry analysis was performed to identify the % positive population of nestin (A), STRO-1 (B), vimentin (C), α-smooth muscle actin (D), fibronectin (E) and cell proliferation marker ki67 (F) in isolated hBMSCs (N=3).

3.4.3. Gene and protein expression of stemness markers in isolated hBMSCs

To validate purity and stemness of hBMSCs isolated from the bone marrow of human subject, protein expression and gene expression of stem cell marker (multipotent and pluripotent) and a mesenchymal marker were monitored by western blotting and real-time PCR analysis respectively.

A. Protein Expression (Western Blot):

hBMSCs (P#3-5) isolated from six different human subject donor's bone marrow, which was subjected to protein harvest for monitor protein expression of cluster of differentiation (CD) markers i.e. CD44 and CD105 which is exclusive MSC marker. hBMSCs samples from all six patients were positive for CD44 and CD105, however, these markers were comparatively low in one human subject's hBMSCs sample (Number:4). Mesenchymal markers like vimentin, α-SMA, and fibronectin were firmly expressed in all hBMSCs samples. The presence of adult stem cell markers such as β-catenin and SOX2 in all samples confirmed the stemness of the hBMSCs (Figure:3.6).

B. Gene Expression (qPCR):

Subsequently, we tested these cells for the presence of all pluripotent stem cell markers at transcript (m-RNA) levels by quantitative real-time PCR (qPCR) on hBMSCs. Gene expression profile of all stem cell markers like *c-MYC, KLF-4, OCT-4, SOX2,* and *NANOG* was carried out. These marker profiles for *NANOG, OCT-4, SOX2, KLF-4,* and *C-MYC* detected by qPCR indicated the pluripotency of hBMSCs. Here, we represent real-time PCR results in delta C_T, which indicate higher C_T values illustrate low gene expression and vice-versa. Based on this fact, we found out that amongst all *C-MYC* showed higher expression and *NANOG* exhibited lower expression while others gene *OCT-4, SOX2, KLF-4* exhibited moderate gene expression in hBMSCs (Figure:3.6).

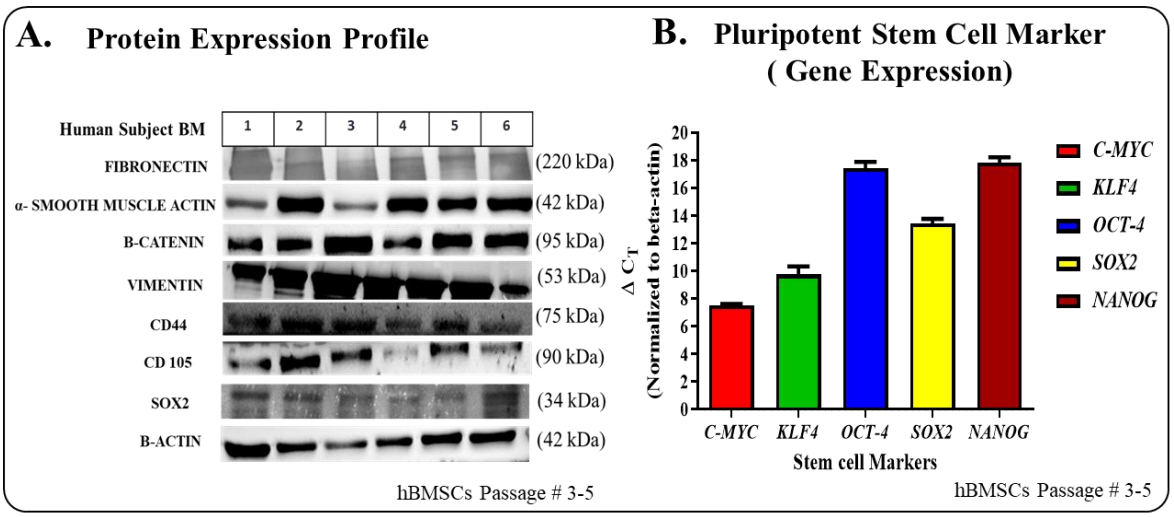

Figure 3. 6: Gene expression & protein expression of stemness markers in patient-derived hBMSCs. (A) western blotting profile of hBMSCs represents human subject-specific protein expression of MSC, mesenchymal marker, and pluripotency [β-actin used as endogenous control].

(B) The expression level of the various pluripotent gene (*C-MYC, KLF-4, OCT4, SOX2, NANOG*) by qPCR (qPCR data represents in Delta C_T; normalized with β-actin as endogenous control). The graphs are plotted with mean ±SEM (N=6).

3.4.4. Trilineage differentiation potential of hBMSCs:

hBMSCs are characterized as a multipotent stem cell that should be able to differentiate to distinct lineages such as adipocytic, chondroblast, and osteoblastic (Xu *et al*. 2017). Therefore, further characterization was performed by differentiating the isolated hBMSCs toward tri-lineages.

A. Adipocyte differentiation:

hBMSCs were differentiated into adipogenic cell type nearly after 21 days of incubation in adipogenic induction specific medium. Adipocytic induction in this hBMSCs was signed by the alteration in morphology of cells from spindle-shaped to round to oval-shaped and by the presence of abundant large, round intracytoplasmic lipid-oil droplets. These lipids (oil) droplets were stained red (positive) with Oil Red O stain post adipogenesis and were very significant in differentiated cells as compared to undifferentiated hBMSCs (Figure No: 3.7).

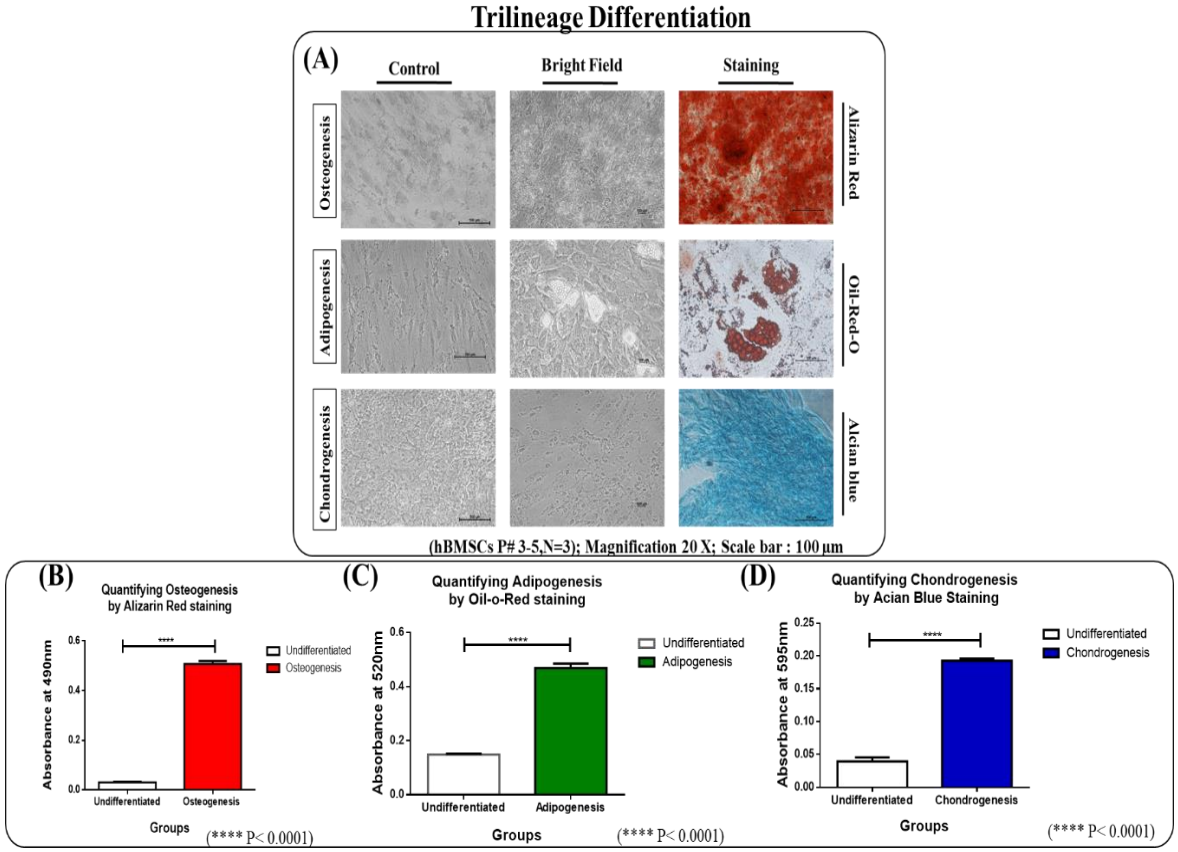

Figure 3. 7: Differentiation of hBMSCs to trilineage differentiation. (A) hBMSCs were induced for osteogenic, adipogenic, and chondrogenic differentiation and finally confirmed by staining with respective dyes with Phase contrast microscopic. Additionally, comparative, statistical analysis of the extent of multilineage differentiation is demonstrated by graphs of extracted stains from undifferentiated hBMSCs and differentiated cells from osteogenesis, adipogenesis, and chondrogenesis respectively (B, C, D). The graphs are plotted with mean ± SEM **** P≤ 0.0001 undifferentiated hBMSCs vs differentiated hBMSCs (The data shown are representative of three independent experiments; N=3).

B. Osteocyte differentiation:

hBMSCs differentiated into osteogenic cell lineage after 21 days of incubation in an osteogenic promoting medium. The osteogenic phenotype in induced hBMSCs was signed by the transition in cell structure, from spindle-shaped to cuboidal, and by the deposits of calcium phosphate mineral. An excessive amount of mineral around the cell surface was observed on day 21 of differentiation. This mineralization was confirmed by staining with Alizarin Red S dye which stains the calcium deposited by differentiated osteocyte and the staining for osteogenesis was highly significant when compared to undifferentiated hBMSCs (Figure:3.7).

C. Chondrocyte differentiation:

Similar to osteogenic and adipogenic differentiation, hBMSCs differentiated into chondrogenic cell lineage after 21 days of incubation in a chondrogenic defined medium. The chondrogenic phenotype was signed by the gradual changes in cell morphology, from spindle-shaped to larger round cell assembles, and by the store of sulfated proteoglycans which are existing in cartilage. These proteoglycans in the matrix stained depict with alcian blue. Post differentiation staining for chondrogenesis was significant when compared to undifferentiated hBMSCs (Figure:3.7).

All these data presented for flow cytometry, immunocytochemistry (ICC), western blotting, qPCR, and trilineage differentiation provided us substantial pieces of evidence that hBMSCs are possessed mesenchymal stem cell characteristics and its potential to differentiate into osteogenic, chondrogenic and adipogenic lineage post isolation and propagation in the culture condition.

3.4.5. Differentiation of hBMSCs into ILCCs (10th Day protocol; Non-adherence plates)

Swertisin is a key small bioactive molecule ingredient isolated from the methanolic extract of *Enicostemma Littorale*. Its islet differentiation potential, as well as the protocol, has been well established in mouse BMSCs, PANC1, rat IPC, NIH3T3, and mouse PREPs (Gupta *et al.* 2010, Dadheech *et al.* 2013, Srivastava *et al.* 2019). Hence, we aimed to extrapolate the islet differentiation potential of swertisin in hBMSCs. Thus, well-characterized hBMSCs were differentiated in four different culture condition group: SFM, SFM +ITS, bioactive molecules cocktail (In which key bioactive molecule "swertisin") and activin A. Differentiation was done at passage 3-6 in 6-well non-tissue culture treated plate (non-adherent plates) by taking an equal number of hBMSCs in each group. Activin A was kept as a positive control which is a known differentiating agent. The insights from the published lab reports suggested that swertisin was capable of differentiating mouse BMSCs into ILCCs in 10 days. Hence, in initial sets of islet differentiation experiments, we monitored the islet differentiation process of hBMSCs till 10 days to assess if the formation of cell clusters which is the foremost mandatory step for islet formation is taking place or not. Microscopic examination and DTZ staining confirmed ILCC formation by 10th day (Figure:3.8). Further, we also settled on some critical parameters before and during islet differentiation such as initially cell seeding density and scheduling trypsinization. Both too long or too short dissociation process can cause the failure of cluster formation, thus significantly reducing the number of cells forming clusters.

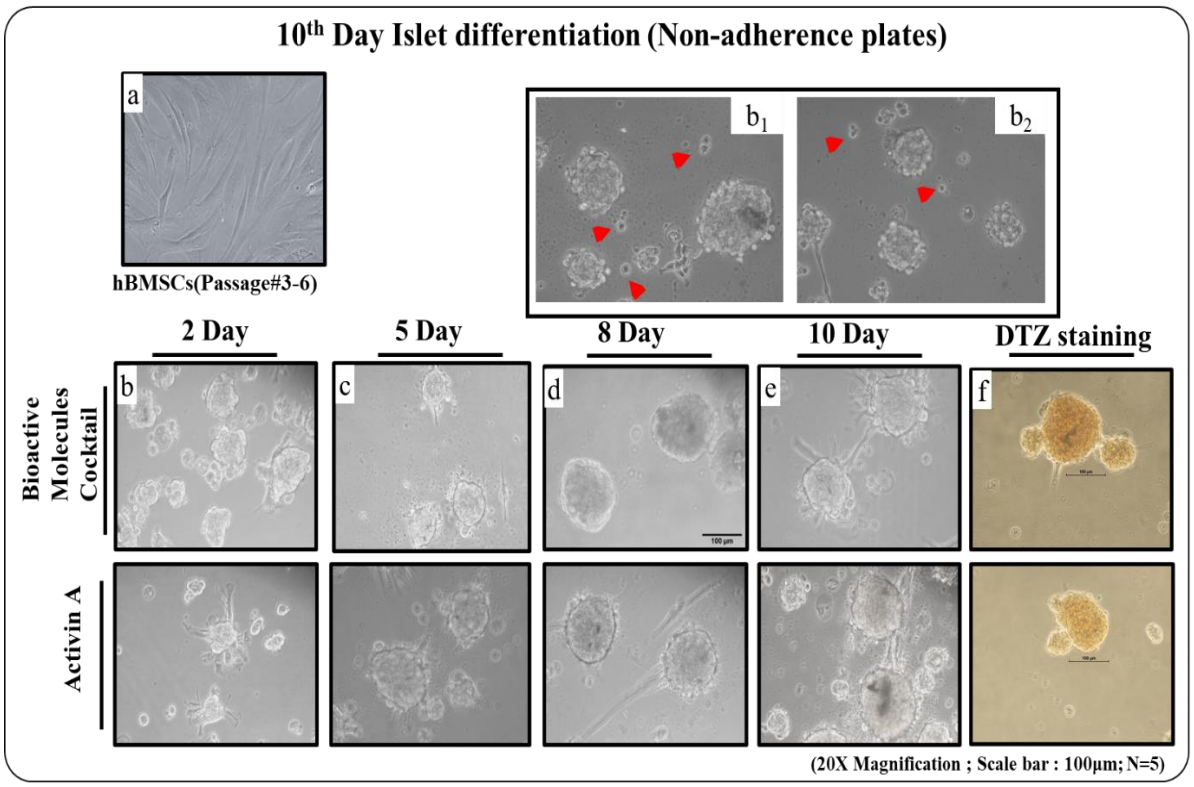

Figure 3. 8: Differentiation of hBMSCs into ILCCs (10 Day protocol). Phase-contrast microscopy of ILCC at different stages (2 Day, 5 Day, 8 Day, 10 Day) of islet differentiation process (activin A positive control group, hBMSCs at P#3-6 as undifferentiated hBMSCs (a); some of the non-participating undifferenced hBMSCs (single cells) /cluster (Arrow indicate by a red arrow) adhered to the culture dish bottom and reminded as non -contribute cells in course of islet differentiation. DTZ staining was performed on 10th day (Five independent observations; N=5).

However, during the differentiation process, we observed some roadblocks such as:

1) Many irregular cell clusters were formed during islet differentiation.

2) Some of the cells adhered to the surface and thus not participate in cluster formation till the end of the islet differentiation process.

3) Although the ILCCS in the BMC and activin A group were positive for DTZ staining as compared to non-differentiated cells but was not very intense.

4) The low insulin transcript level was obtained on 10 days of islet differentiation from hBMSCs [Figure:3.10(B)]

Thus, the 10 days of islet differentiation attempt gave the insight that in spite of being of mesoderm origin, we could successfully differentiate the hBMSCs into endodermal lineage to form islets. Accordingly, we next focused on pinpointing the drawbacks as mentioned above

by strategically modifying the differentiation protocol in various steps. [Note: since SFM and ITS group had small cell clusters with incomplete differentiation, we phase out these two groups in further experiments (Figure:3.9)]. During the differentiation process, we stepwise operated and overcame the hurdles to gain the best strategy to make functional ILCCs.

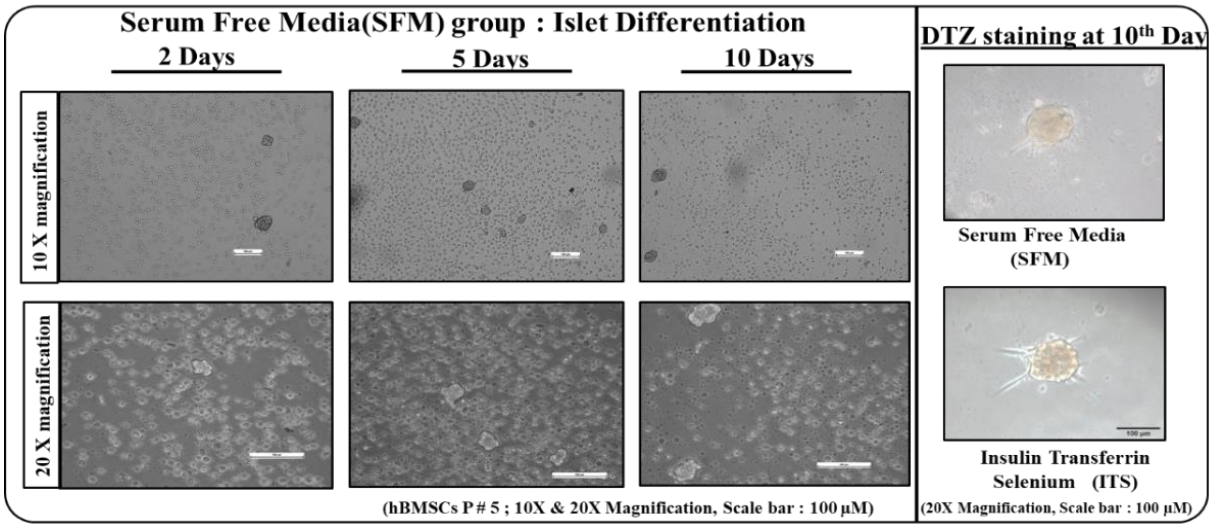

Figure 3. 9: Phase contrast microscopy of cell clusters at different stages (2 Day, 5 Day, 10 Day) of the islet differentiation process in serum-free media (SFM). A very small loose cluster was formed in serum-free media induction. DTZ staining was performed in SFM and ITS cell clusters on 10th day (N=3).

3.4.6. Differentiation of hBMSCs into ILCCs (18th Day protocol; non-adherence plates)

As stated previously that the DTZ staining and insulin transcripts were underachieved in 10 days of differentiation, we extended & switched to 18-day islet differentiation protocol. This time point was further supported by the protocol published by (Yu *et al.* 2007, Czubak *et al.* 2014, Gabr *et al.* 2014) . In order to increase the participation of the cells in the differentiation and to improve cell survival during the process, we introduced additional differentiating factors/ growth factors during the process. The pancreatic islet differentiation was induced by a systematic four-multi stage treatment of retinoic acid, hepatocyte growth factors (HGF), fibroblast growth factor (FGF), epidermal growth factor (EGF) along with some growth supplements (B-27 and N-2), and chromatin remodelling factor (sodium butyrate). Additionally, in later stages of islet differentiation, we augmented the differentiation process with nicotinamide and exendin-4 for enhancing insulin-production. These modifications in differentiation media lead to cell migration towards a central zone to form spherical shape

pancreatic islet morphology within 24 hours of supply of induction media. After extending the differentiation period from 10 to 18 days, DTZ staining was more intense corresponding to higher insulin levels in cells.

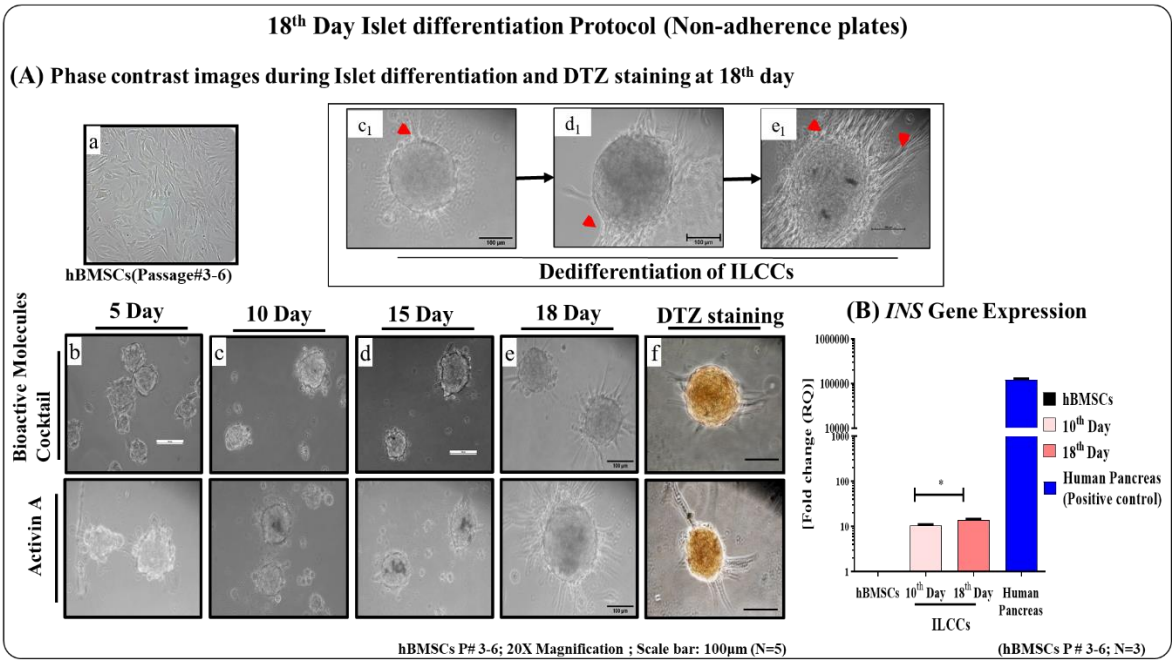

Figure 3. 10: Differentiation of hBMSCs into ILCCs (18th day protocol- non-adherent plates). (A) Phase-contrast microscopic images during islet differentiation (a) undifferentiated hBMSCs; many asymmetrical clusters formed in the first stage of induction at 5th day (b), develop compact clusters in the second stage of induction at 10th day (c), and became spherical with blurred boundaries among adjacent cells in the third stage of induction at 15th day (d), while some of the formed clusters/ single cells adhered to the culture plates bottom and cells started migrating from settling down clusters (stage viz representative images c_1,d_1,e_1) and ultimately its started dedifferentiation at 18th day induction (e). The majority of cell clusters settled down during islet differentiation after 10th day induction stages and always adhered to the dish bottom (N=5). DTZ staining was done at 18th day ILCCs and showed remarkably positive red color in both groups (f). (B) Human Insulin Gene expression by qPCR for day 10 ILCCs (previous 10th protocol), day 18 ILCCs (Current 18th day protocol), human total pancreas (as experimental positive control), and hBMSCs (as experimental negative control) * $P \leq 0.05$ (10th day protocol ILCCs vs 18th Day ILCCs).The graph is plotted with the mean ±SEM of three independent observations (N=3).

Although higher insulin expression was successfully achieved, we examined two very crucial phenomena in both groups (activin A and BMC) during islet differentiation:

(1) During the progression of differentiation, at a later time point, some of the cell clusters displayed central necrosis (Figure No: 9 & 10).

(2) Most of the cell clusters got settled down into the bottom of the plates. This hampered the yield of fully mature islets and also caused some ILCCS to de-differentiation. Importantly, this adherence to surface resulted in difficulty in the picking of ILCCs for later experiments such as transplantation (Figure:3.10).

To address and overcome central necrosis problem, curcumin (a known anti-apoptotic and antioxidant bioactive molecule) was added in the last stage of islet differentiation. The effective dose of curcumin on hBMSCs [Figure No: 3.11(a)] was obtained as 10 µM (Meghana *et al.* 2007). Also, we confirmed that alone curcumin (10 µM) treatment resulted in very loose cluster / no cell cluster formation and hence was insufficient to differentiate hBMSCs to ILCCs [Figure: No:3.11(b)]. However, cell clusters in BMC treated with curcumin demonstrated remarkably reduced central necrosis in cell clusters during islet differentiation, thus potentiating the healthy islet yield due to curcumin's anti-apoptotic and antioxidant properties.

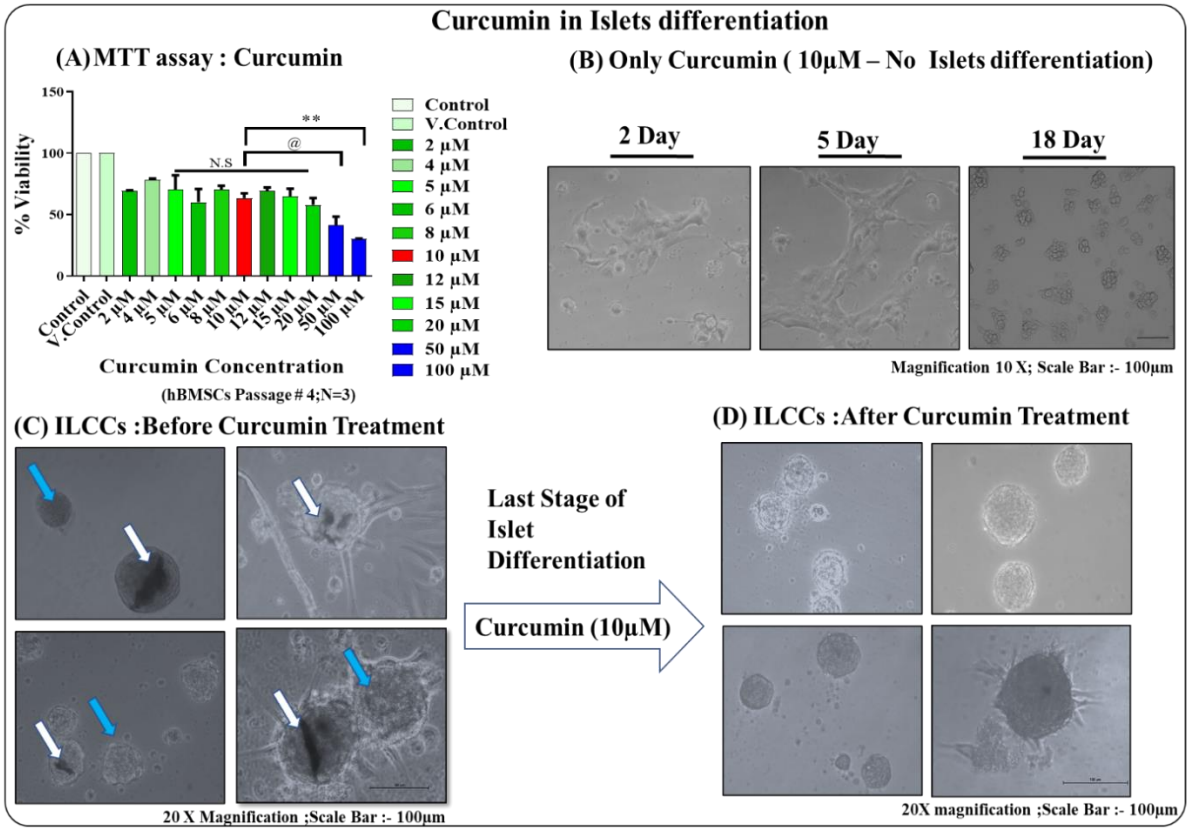

Figure 3. 11: Curcumin reduced central necrosis during islet differentiation. (A) the cell viability was determined by MTT assay in hBMSCs with a range of curcumin dose (2 µm to 100 µm). 10 µm conc. of curcumin showed slightly reduced viability but significantly increased cell viability as compare to 50µm and 100µm conc. of curcumin. No significant difference was observed

between 5 µm to 20 µm conc. of curcumin. 10 µm conc. of curcumin vs 100 µm conc. of curcumin ** P ≤ 0.01; 10 µm conc. of curcumin vs 50 µm conc. of curcumin @ P ≤ 0.05. The graph is plotted with a mean ±SEM (B) Phase contrast microscopic image of islet differentiation in the presence of 10 µm conc. of curcumin. hBMSCs didn't participate in cell cluster formation in the presence of curcumin (C) Representative image of phase contrast microscopic of differentiated islets shows central necrosis without curcumin treatments (White arrow indicates "Necrotic ILCCs" while blue arrow indicates "without necrotic ILCCs"). (D) Phase-contrast microscopic show that after curcumin treatment remarkably reduced central necrosis in ILCCs (N=3).

3.4.7. Differentiation of hBMSCs into ILCCs (18th Day protocol; ultra-low adherence plates) * (Entire islet differentiation protocol is filed for Indian Patent)

After addressing the central necrosis problem, our second hurdle was the ILCCs adhering to the surface. hBMSCs have an inherent property of adhering to any surface they come in contact with, to avoid which plates noticeably managed to maintain a constant floating 3-dimensional ILCCs (3D-ILCCs) culture throughout the islet differentiation (Figure: 3.12).

We faced one more issue like cell clusters aggregating with each other's during the process of islet differentiation due to applying ultra-low adherence (ULA) culture plates (Corning, USA) for suspension culture. During the islet differentiation process, we noticed that after 2-3 days of islet differentiation, generally 4-6 number of clusters (similar size and weight) start merging with each other's and formed a single large cell cluster (Figure: 3.12). Due to the merging of cell clusters, central necrosis is elevated and eventually affect pancreatic islets function along with yields. To overcome this issue, we decided to shake culture plates forward and backward (Manually) every alternative day after cell cluster formed. To the relief, the shaking drastically reduced cell cluster merging problem and obtained well-separated cell clusters with a great yield at the end of islet differentiation (Figure: 3.12).

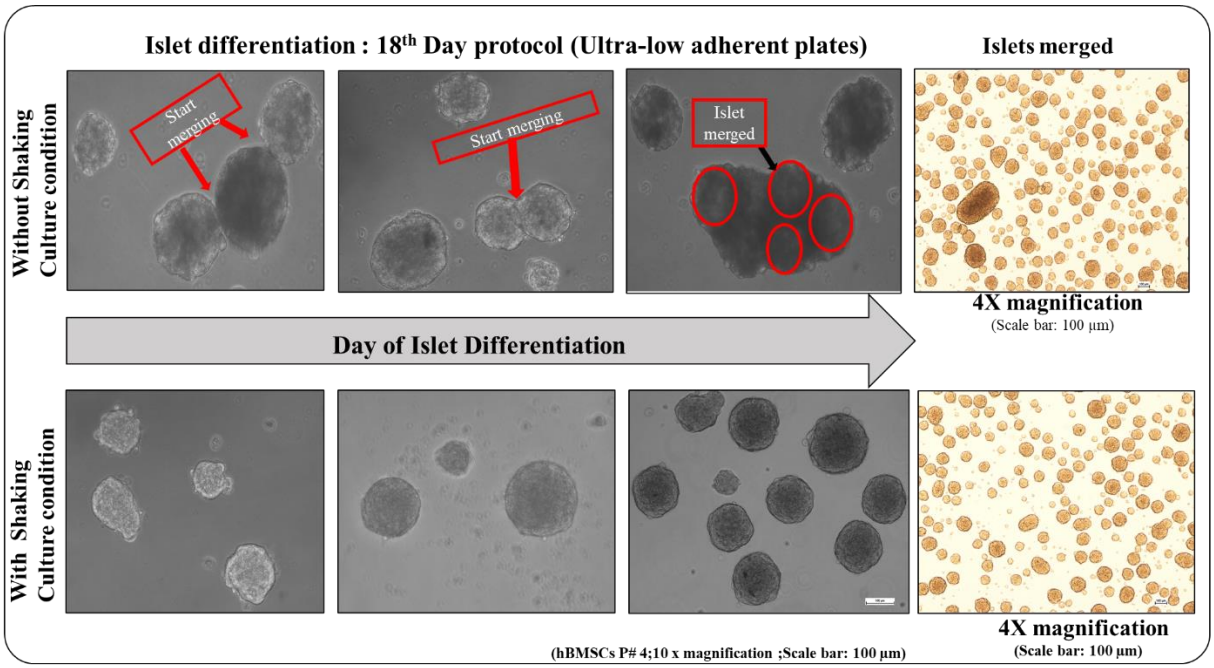

Figure 3. 12: Schematic representation of phase contrast microscopic of differentiated ILCCs was getting merged during islet differentiation. Due to the use of ultra-low adherent plates, differentiated cell clusters were prevented for settling down to plates bottom and staring merged with each other during the course of islet differentiation in without shaking culture condition (shown by red arrow/ circles in an above panel). While during shaking culture conditions, the majority of cell clusters prevented from getting merged. We also captured an expended outlook in 4 X magnification (Three independent observations N=3).

To study cell assembly kinetics, 3D cell cluster formation was monitored at different time-points (5^{th} day,10^{th} day,15^{th} day,18^{th} day) as shown in figure number 3.13. The results demonstrated the cluster formation with blurred boundaries within 24 hours of cell seeding, and close-fitting 3D clusters were obtained subsequently 5 days of culture which remained stable in size until the end of the 18^{th} day differentiation period. These 3D-ILCCs were subjected to DTZ and were intensely stained (Crimson red) positive in activin A and BMC group indicating the presence of a large number of insulin-containing vesicles. Also, the staining color intensity was visibly much better in the BMC group as compared to the activin A group (Figure: 3.13). This allowed us to infer that we could settle on the differentiation protocol for hBMSCs to islets of 18 days incorporating ultra-low adherence, curcumin treatment, and shaking culture conditions to obtain the best possible yield of ILCCs. Hence, the present optimized islet differentiation protocol was selected for further experiments.

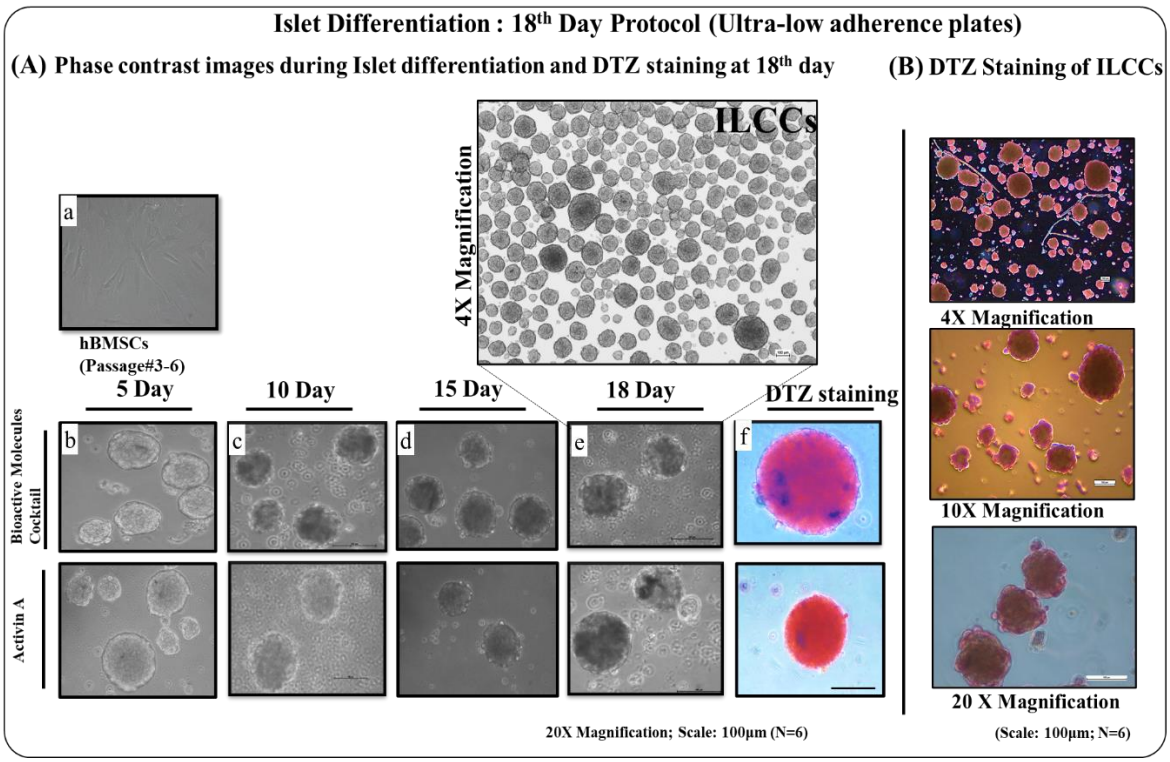

Figure 3. 13: Differentiation of hBMSCs into ILCCs (18th day protocol- Ultra-low adherent plates). (A) phase-contrast microscopic images during the islet differentiation process. Representative undifferentiated hBMSCs shows a fibroblast-like morphology (a), After induction, within 24 hrs. of a short time, rapidly cell clusters formation with a maximum number of cell participation (b), in the second stage of induction, cell clusters formed more tight spherical shape with a negligible amount of cell clusters adherent to plate bottom(c), the third stage of induction showed clear periphery of a tight cluster (d), the last stage of induction demonstrates prominent close-fitting cell clusters, analogous to the morphology of islets (e), most of the 18th day ILCCs stained with deep crimson red DTZ staining for primary confirmation of β-cell differentiation (f).In both groups (BMC and activin A) showed the very similar morphological appearance of undifferentiated hBMSCs into ILCCs formation. (B) DTZ staining of 18th Day ILCCs (BMC) showed strongly positive DTZ staining (intense crimson red color) with different magnification (N=6).

We also calculated and compared the total yield of ILCCs between non-adherence and ultra-low adherence groups. We found out that the ultra-low adherence (ULA) induction group showed a significantly high yield of ILCCs as compare to the non-adherence induction group. No significant differences were observed between the activin A and the BMC group (Figure: 3.14).

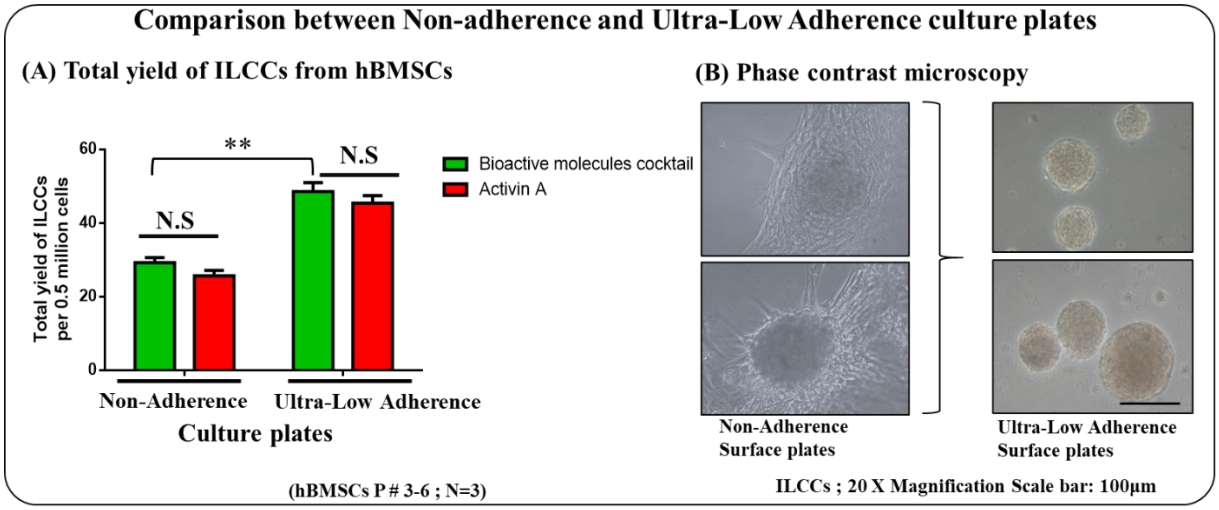

Figure 3. 14: Analysis of total yield of ILCCs from hBMSCs using phase-contrast microscopic. (A) Total ILCCs yield was counted per 0.5 million hBMSCs for both groups in different culture plates such as non-adherent and ultra-low adherence (ULA) plates. Significant higher ILCCs were observed in the ULA plate for both groups (activin A and BMC) whereas, no significant difference was found between activin A and BMC group in case both non-adherent and ULA plates. Approximately, 50 ILCCs generated from hBMSCs in ULA plates in both groups. **P ≤ 0.01 (non-adherent plates vs ULA plates in BMC group). Experiments are performed in triplicate and data are depicted as the mean ± SEM (B) Representative images of ILCCs in non-adherent and ULA plates. In ULA plates, the majority of 3D cell clusters were formed in suspension while, in non-adherent plates, some of the cell cluster attaches to the bottom of plates, and spread out, ultimately reduced total yield of ILCCs (N=3).

3.4.8. Morphometry analysis of differentiated ILCCs

To visualize 3D-ILCCs inside these ultra-low plates, we measured the aggregate diameter of ILCCs on 18th day. We carried out morphometry analysis to segregate Day18 ILCCs into three size groups: <100µm, 100-300µm, and >300 µm, this was compared with control clusters made using activin A as the positive differentiating agent (Figure:3.15). We identified a significant difference between activin A and BMC samples for both <100 µm and >300 µm size group. While no significant difference was observed between activin A and BMC sample in 100-300 µm size group. 60% of the clusters from the test group BMC were <100µm in size which was a positive indication as it has recently been found that Insulin secreting capacity of clusters in a size range below hundred is better than the medium or the large-sized clusters. On another side, only 10 % ILCCs showed higher than >300 µm size of islets in the BMC group while approximately 20 % ILCCs were observed in activin A group. After morphometry analysis,

microscopic evaluations on the ILCCS stained with fluorescein diacetate (FDA)/propidium iodide (PI), and quantitative analysis of apoptosis was performed by FACS (Annexin V/PI).

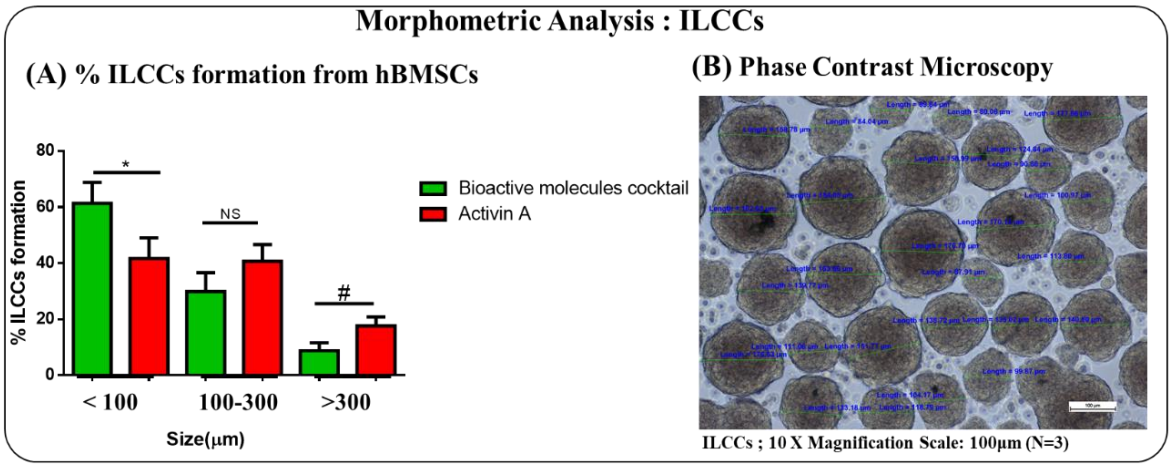

Figure 3. 15: Morphometric analysis of hBMSCs generated 18th Day ILCCs. (A) Phase-contrast microscopic analysis was carried out to segregate ILCCs into three size group: <100 µm(small), 100-300 µm(medium) and >300 µm (large), this was compared between ILCCs generated from hBMSCs using BMC and activin A. Insulin secreting capacity of clusters in a size range below hundred is better than the medium or the large-sized clusters and our results demonstrated that 60% of the clusters from the test group (BMC) were <100µm in size.*P ≤ 0.05 (BMC compare with activin A in <100 µm size group); # P ≤ 0.05(BMC compare with activin A in >300 µm size group). No significant difference was observed between both groups in 100-300 µm size of ILCCs. Results are demonstrated as mean ± SEM of three independent observations (N=3). (B) Representative image of ILCCs size measured using microscopic image analysis software (NIS Elements BR, Nikon).

3.4.9. Cell viability assay: 18th day ILCCs

The FDA/PI staining was performed on 18th Day ILCCs for confocal microscopic evaluation of differentiated islets viability. In this assay, viable ILCCs exhibited green and dead cells presented red fluorescence. The widely stained green color regions are related to the FDA-stained (live) ILCCs. The tiny bright spot in the fluorescent images correlates to the deep red staining of the PI-positive population (dead) in ILCCs. In the BMC group, ILCCs stained with FDA/PI show a high level of green fluorescent and low level of red fluorescent that may be due to the antioxidant activity of BMC (Figure:3.16). Further, this data was validated with apoptosis assay using Annexin V- PI staining through flow cytometry analysis.

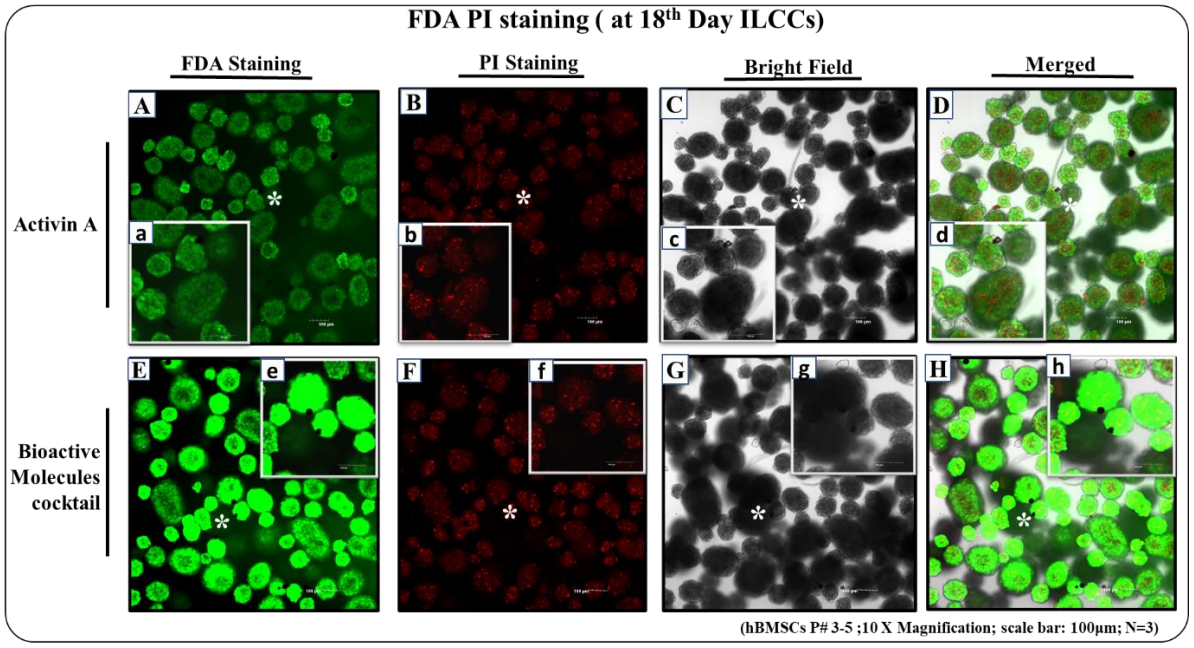

Figure 3. 16: Live /Dead staining with FDA/PI dye at 18th Day ILCCs by confocal microscopy. BMC group showed remarkable higher signal (indicate more viability) with FDA dye (E and e) as compare to activin A group (A and a), whereas both groups showed obscure signal difference (less death) with PI dye (B-b & F-f) [White asterisks (*) denote regions enlarged in corner of each image]. Merged image (FDA/PI/ bright field) showed combine live /dead cells in both groups. (D-d, H-h) ; Scale bars: 100µm (N=3).

Apoptosis was quantified by flow cytometry analysis after staining with Annexin V and PI at the end of the islet differentiation (day 18). Figure: 3.17 shows the percentages of Annexin V-PI-stained cells of differentiated ILCCs. BMC group showed less apoptotic cell population (35.4 %) as compare to activin A group (43.5 %) due to the presence of bioactive molecules like swertisin and curcumin in the BMC group. Further, we also decided to check cellular ROS status in differentiated ILCCs.

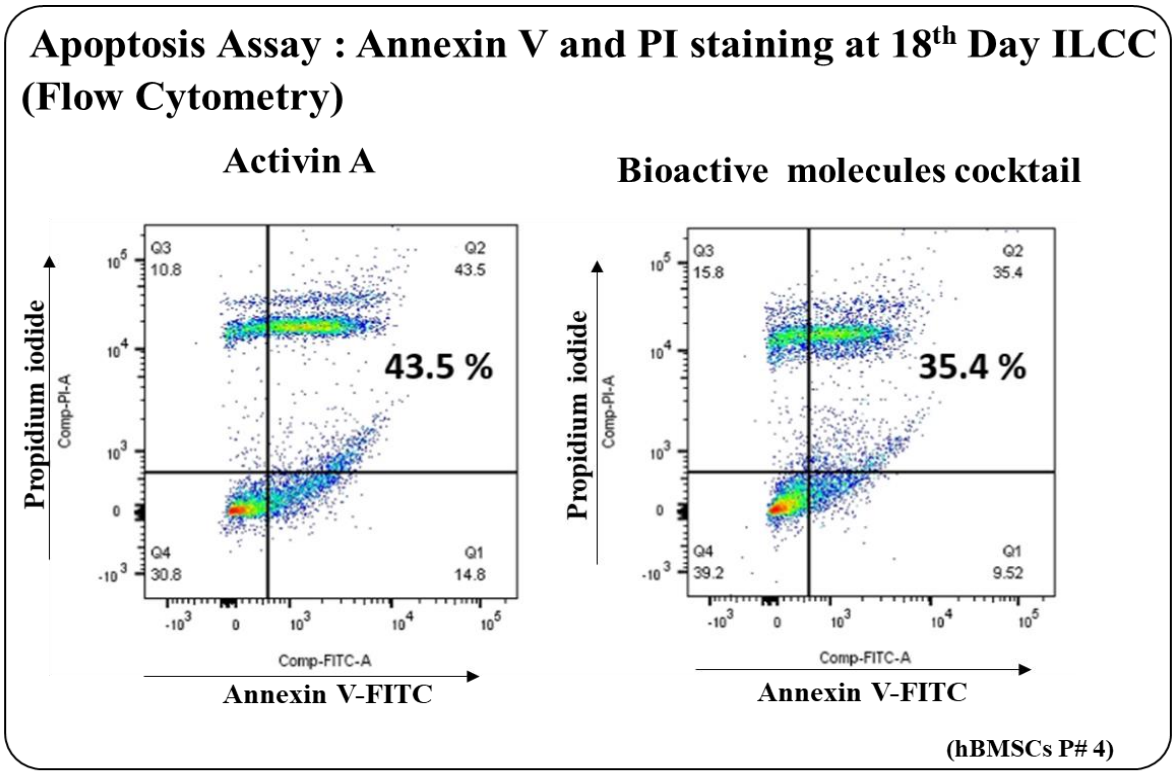

Figure 3. 17: Representative flow cytometry analysis of apoptosis using annexin V and propidium iodide (PI) staining. 18th Day ILCCs of both groups were stained with Annexin-V-FITC/PI. BMC group showed less apoptotic cell population (35.4 %) as compare to activin A group (43.5 %) FITC, fluorescein isothiocyanate; PI, propidium iodide.

3.4.10. Measurement of cellular ROS in 18th day differentiated ILLCs using DCFDA assay:

The BMC group showed significantly lower cellular ROS as compare to the activin A group (Figure:3.18). Additionally, to validate our fluorescence reader data we decided to execute fluorescent microscopy analysis for detecting cellular ROS using the same DCFDA dye in 18th day differentiated ILCCs. Quantitative comparisons of the areas of the green color suggested that percent cellular ROS in samples. We observed that a significantly low level of ROS detected in the BMC group as compare to the activin A group (Figure: 3.18). A cocktail of bioactive molecules containing swertisin, curcumin was used during islet differentiation for protecting ILCCs from cellular ROS and apoptosis.

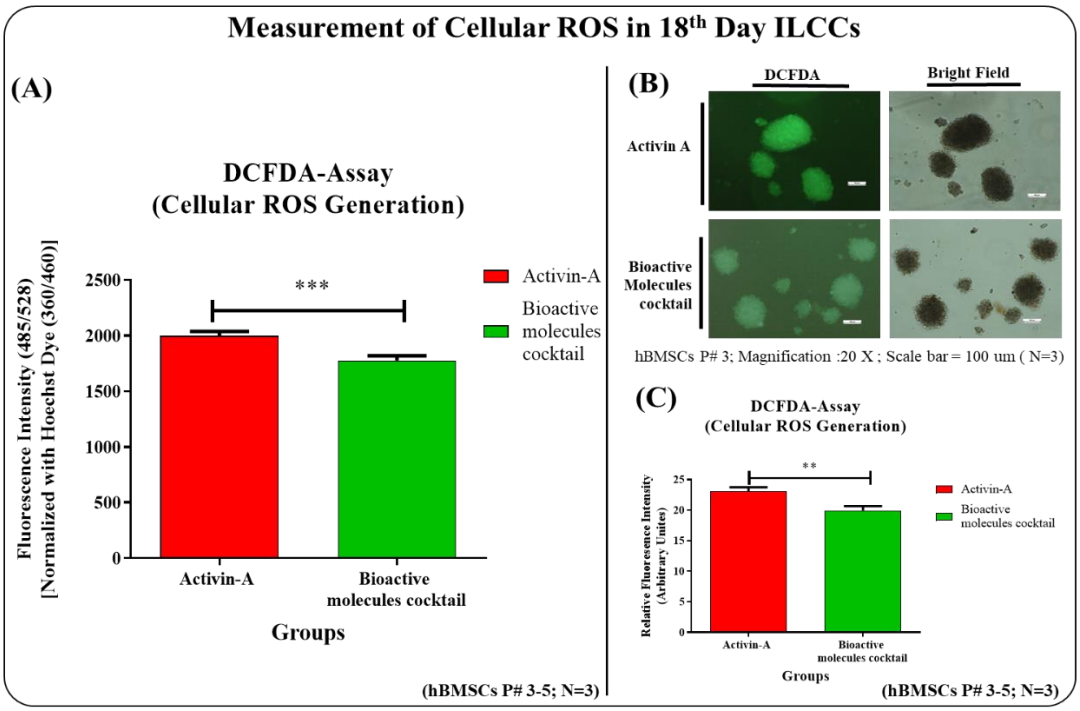

Figure 3. 18: Measurements of cellular (reactive oxygen species) ROS in 18th day ILCCs by DCFDA assay. (A) DCFDA- Fluorescence intensity was measured by a multimode reader to detect cellular ROS in activin A and BMC. The BMC group showed significantly lower cellular ROS as compare to activin A group. Hoechst dye used for the normalization of nucleus content. Experiments are performed in triplicate and data are demonstrated as the mean ± standard error of the mean (SEM) *** P ≤0.001 (activin A vs BMC). (B) Representation of fluorescent microscopic images of DCFDA stain in both groups. The BMC group displayed a noticeable lower DCFDA intensity as compare to activin A group. (C) Additionally, relative fluorescent intensity was calculated based on ILCCs stained with DCFDA fluorescent dye in fluorescent microscopy. Activin A demonstrated significantly higher cellular ROS as compare to the BMC group. Mean ± SEM ** P ≤ 0.01(activin A vs BMC).

3.4.11. Gene expression of lineage-specific markers involved in islet differentiation of ILCCs (by Taq-man)

Using Taq-man Low-Density Array (TLDA), we screened 18-day ILCCs from the test plate as well from the positive control in comparison to undifferentiated hBMSCs for 11 different genes involved in islet development and maturation (Figure:3.19). Out of all the genes screened, definitive lineage-specific markers showed a sharp change in expression. Nestin's expression increased in both day 18 clusters in comparison with hBMSCs indicating and increase in endocrine progenitor cells. Similarly, *NGN3* and *MAFA*'s (marker for β-cell specification) expression was seen to increase in 18-day ILCCs.

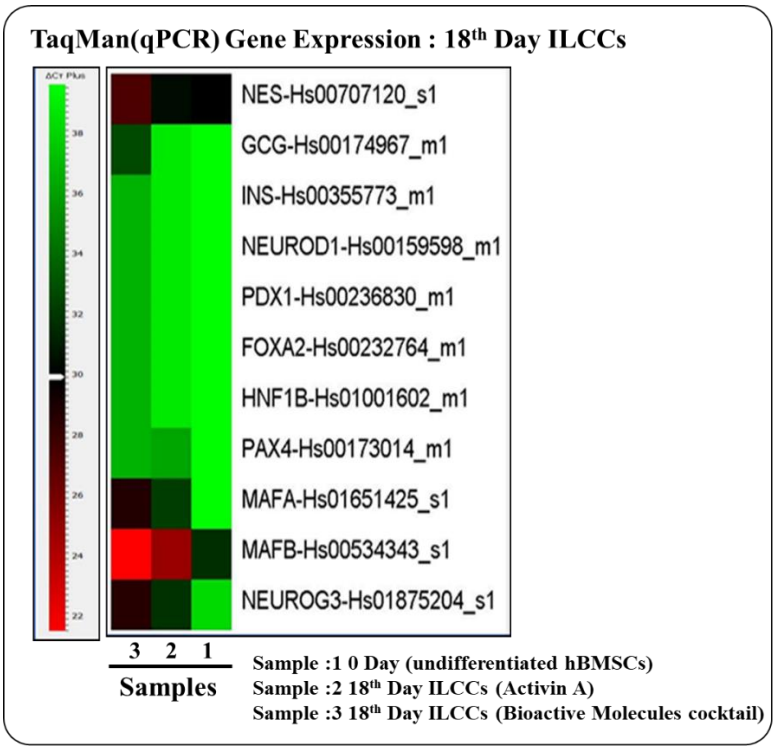

Figure 3. 19: Heatmap displaying the relative gene expression of the top 11 upregulated genes at 18th day ILCCs. Data represent fold change of gene expression determined by Custom designed TaqMan probes and we note that sample names Sample 1: Undifferentiated hBMSCs; Sample 2: Day 18 clusters differentiated with activin A; Sample 3: Day18 clusters differentiated with BMC; Endogenous control: 18S rRNA; For each sample, relative expression was normalized to hBMSCs (Undifferentiated – 0 Day). Color from red to green indicates high to low gene expression. Dark shades indicate higher expression and light shades indicate lower expression (Heat maps generated by Data assist software, ABI, USA) [N=2].

It was observed that ILCC derived using BMC had higher gene expression of *FOXA2* & *HNF1ß* (Marker for definitive endoderm), *NGN3* (Marker for pancreatic progenitors), *PDX1* (essential for pancreatic primordium expansion & islets development), *Nestin* (Endocrine marker), *MAFA* & *PAX4* (expressed in β cells) when compared to gene expression of our positive control i.e. activin A (Figure:3.19). Insulin gene expression was also seen to be high in BMC derived ILCC (Figure: 3.19). The expression pattern of all these lineage-specific genes indicated that hBMSCs induced for differentiation were entering subsequent lineages during the protocol.

3.4.12. Islet functionality of 18th Day ILCCs: Immunocytochemistry

To understand the functionality of the ILCCs formed at day 18 Immunocytochemistry (ICC) was performed using confocal microscopy. The results showed the presence of insulin and

glucagon expressing cells (Figure: 3.20) corresponding to terminal differentiated pancreatic β and α-cells respectively.

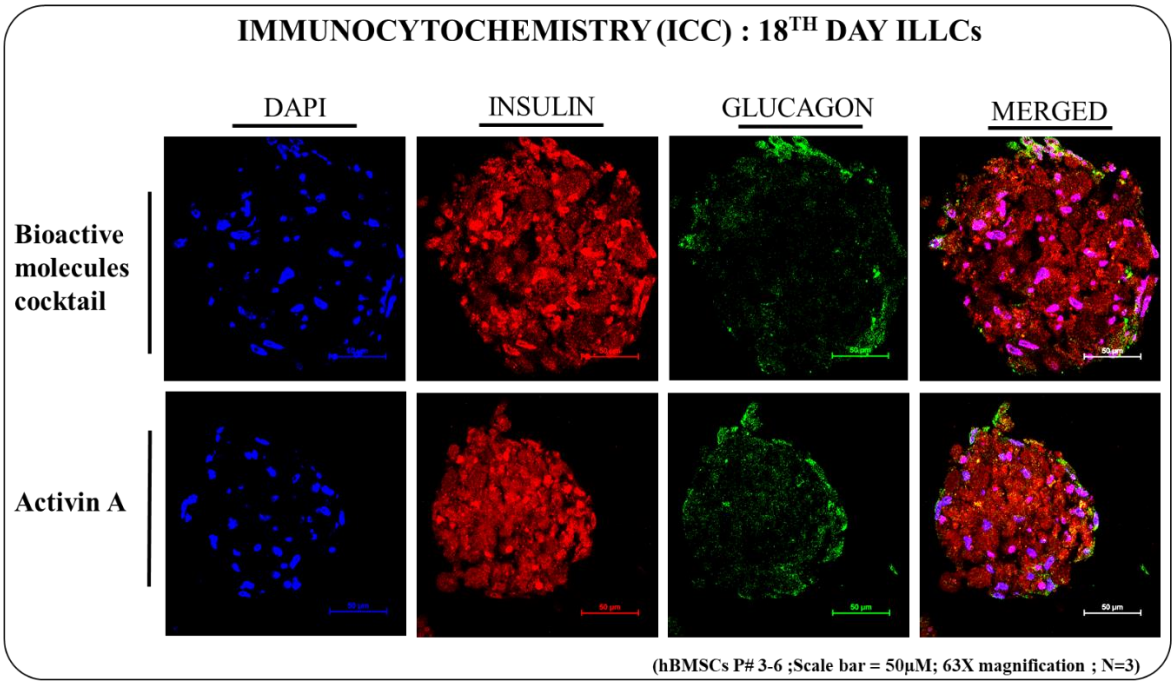

Figure 3. 20: confocal immunocytochemistry of 18th Day ILCCs obtained at the end of the 18th islet differentiation protocol shows the expression of the functional pancreatic marker. Confocal optical sections of ILCCs double immunofluorescence stained for Insulin (Red color- TRITC), which is a β cell-specific marker and glucagon (FITC-Green), which is an α cell-specific marker. Counterstaining of nuclei was done by DAPI (as shown in Blue). Representative merged images are shown for each group; co-localization of insulin and glucagon is in yellow (very less expression) [Scale bar =50 µM; 63X magnification(N=3)].

Co-localization of insulin secreting cells with glucagon secreting cells suggests the presence of bi-hormonal cells. Also, BMC showed comparatively higher insulin and glucagon protein expression to that of activin A group.

These observations confirmed the formation of mature ILCCs synthesizing pancreatic endocrine hormones, which are all necessary for glucose homeostasis in the BMC and activin A groups.

Additionally, to confirm the insulin and glucagon nil expression of undifferentiated hBMSCs at the protein level were assessed by ICC. All the undifferentiated cells were negative for insulin and glucagon expression (Figure: 3.21).

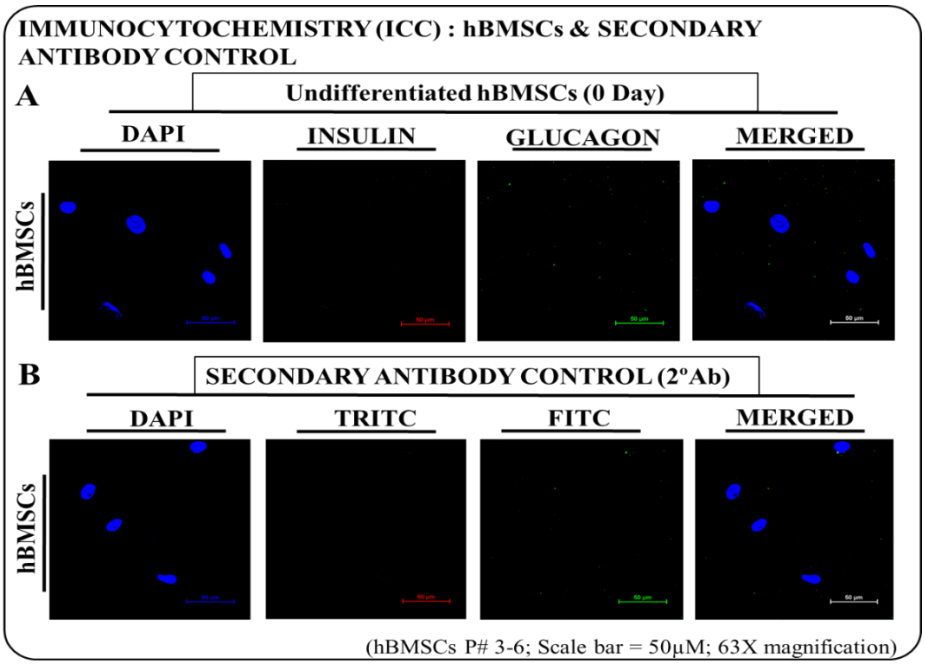

Figure 3. 21: confocal Immunocytochemistry of undifferentiated hBMSCs. (A) The immunocytochemistry image represents nil expression of functional pancreatic islets marker such as insulin and glucagon in undifferentiated hBMSCs. (B) Immunofluorescent analysis of both 2°A control (TRITC, FITC-negative control) was performed in the absence of primary antibody (bottom panel, representative of hBMSCs). Insulin and glucagon images of both groups ILCCs (activin A and BMC) were captured under the same acquisition parameters by confocal microscope Zeiss LSM 710 and analysed by software (NIS Elements- AR 5.11.01, Nikon). Nuclei were stained with DAPI (blue).

3.4.13. Flow cytometry analysis of pancreatic hormone expression in ILCCs

To further confirm the functional of ILCC, flow cytometry analysis was carried out to check them for increasing amounts of c-peptide and glucagon protein expression. The graph of flow cytometry analysis (Figure: 3.22) demonstrates the human c-peptide and glucagon expression positive cells within ILCCs. Also, the BMC group showed comparatively higher c-peptide and glucagon protein expression to that of activin A group. The islets produced on 18^{th} day had 77 % c-peptide levels and 16% of glucagon producing cells. Flow cytometry results concluding that differentiated islets in the BMC were perfect resembling human pancreatic islets because human pancreatic islets have 70-80 % insulin-producing β-cells & 15-20 % glucagon producing α cells.

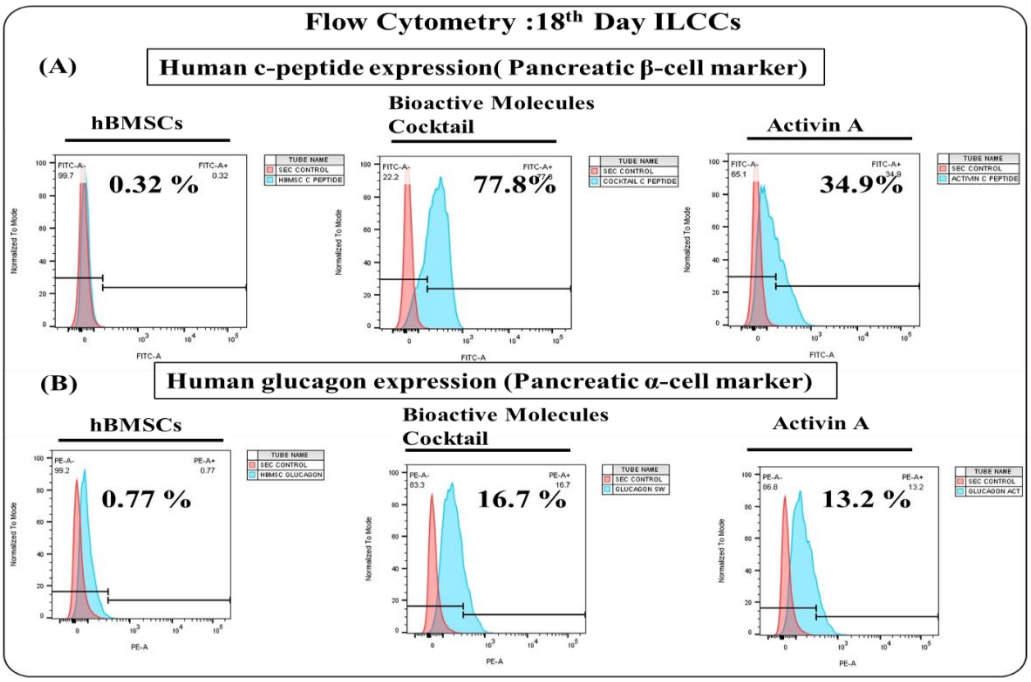

Figure 3. 22: Flow cytometry analysis of functional pancreatic islets marker in 18th day ILCCs. (A) Representative FACS analysis shows that ILCCs was elevated expression of c-peptide in BMC group (77.8 %) as compare to activin A group (34.9 %), while a negligible difference of glucagon expression in BMC group (16.7%) and activin A group (13.2 %). hBMSCs shows almost nil expression of both c-peptide (0.32 %) and glucagon (0.77%). Isotype matched 2°Ab control (FITC- Human c-peptide; PE(TRITC)- Glucagon) was used to eliminate background staining.

3.4.14. *In vitro*: Human C-peptide release in response to a glucose challenge

Further, the c-peptide release assay performed glucose challenge which indicated (Figure: 3.23) that the ILCCs from BMC and activin A groups, all release human c-peptide at a significantly higher level than those of the undifferentiated hBMSCs group. The results also indicated that the c-peptide release of ILCCs in response to glucose challenge occurred in a concentration-dependent manner Further, the BMC group showed significantly higher c-peptide release in 25 mM glucose and 30 mM KCl challenge as compare to activin A group. While BMC and activin A group showed no significant difference in the presence of 5 mM glucose concentration. Thus, our results indicated that matured ILCCs could significantly produce more human c-peptide compare to undifferentiated hBMSCs. Although dynamic human c-peptide release assay showed a more sustained secretion during high glucose in ILCCs compared to hBMSCs, stimulation indices were found to be similar with some minor variation between the three BM donors (Figure: 3.23). So, this confirmed that the islet generated using a BMC and activin A was mature and completely functional. Taking all these results into consideration along with

the results from gene expression, ICC, FACS, DTZ staining, c-peptide ELISA, we could finally conclude that our novel islet differentiation protocol was successfully differentiating hBMSCs into ILCCs.

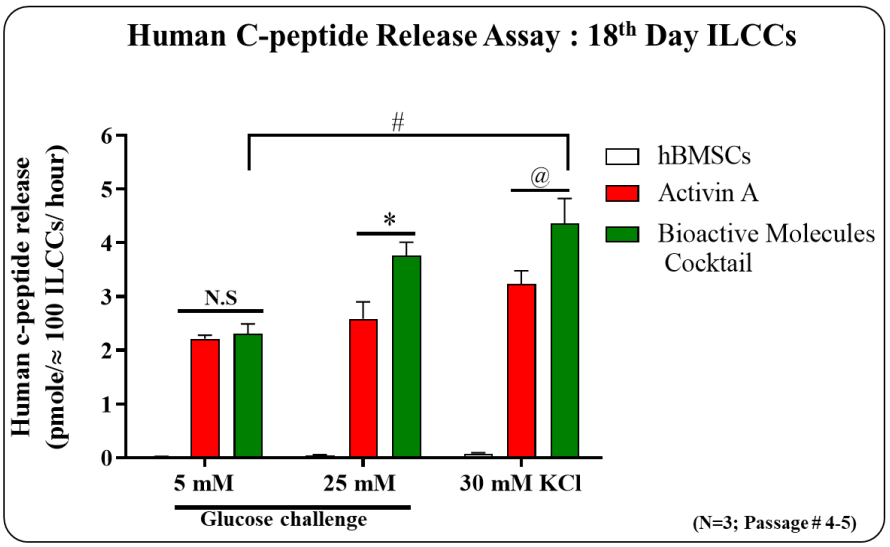

Figure 3. 23: *In-vitro* functional characterization of differentiated 18th day ILCCs by human c-peptide release assay (Chemiluminescence based ELISA, ALPCO, USA). Approximately 100 handpick ILCCs from both groups (activin A and BMC) were sequentially treated with low glucose (5 mM) and high glucose (25mM) conc. as well as 30 mM KCl challenge in triplicate for 1 hrs. 25 mM and 30 mM KCl treatment group showed significant high c-peptide release in BMC as compare to activin A experimental group. No significant difference was observed in activin A and BMC with 5 mM glucose treatment. Error bars represent Mean ± SEM * P ≤ 0.05 (25 mM glucose conc., activin A vs BMC); @ P ≤ 0.05 (30 mM KCl conc., activin A vs BMC) # P ≤ 0.05 (BMC with 5 mM glucose conc. vs 30 mM KCl conc.). Undifferentiated hBMSCs showed a nil amount of c-peptide release (N=3).

3.5. Discussion

In recent years, stem cell advancement in the field of regenerative medicine is interested in β-cell differentiation from different sources of adult stem cells. Despite their promising islet differentiation potential, there are still some vital facts, such as a potent source of stem cells, the efficacy of differentiation (increase islets yield), the functionality of newly generated islets in terms of insulin synthesis and secretion along with enhanced stem cell participation. There is an inadequacy of systematic study to overcome the scarcity of potent differentiating agents and the bioactive molecules as well as the insights of possible combinations of bioactive molecules to get an encouraging yield of functional islets. *In vitro* islet differentiation aims to develop islets that can be transplanted into diabetic patients. Several groups have shown *in*

vitro islet differentiation successfully (Dennis *et al.* 2002, LOPEZ *et al.* , Zeng *et al.* 2016), but there is a lot of room for functional enhancement before these islets like clusters can be transplanted. Not much evidence exists to support the idea that hBMSCs is appropriate for use in clinical transplantation (Milanesi *et al.* 2011, Zanini *et al.* 2011). Thus, in the current investigation, we made an effort to answer these all questions by using a unique islet differentiation protocol based on bioactive small molecules that can achieve glucose-responsive ILCCs from hBMSCs.

Several reports suggested that hBMSCs can be differentiated into pancreatic β-cell *in vitro* (Sun *et al.* 2007, Jafarian *et al.* 2014). More importantly, marappagounder et al., (2012) demonstrated that human BMSCs are more promising for differentiating into ILCCs than those from adipose tissue-derived mesenchymal stem cells (Marappagounder *et al.* 2013). Thus, hBMSCs is a gold standard stem cell sources for islet differentiation. hBMSCs derived from diabetic patients can be converted into ILCCs by *in vitro* differentiation and these differentiated ILCCs can be utilized for the treatment of diabetes.

hBMSCs can be confirmed by the presence of the mesenchymal stemness markers CD105, CD 44, CD 90, CD166, CD73 and the lack of markers like CD45, CD34, and CD31 (Dominici *et al.* 2006, Pal *et al.* 2009, Nekanti *et al.* 2010). Accordingly, our immuno-phenotyping results on isolated hBMSCs were positive for CD105 (83.6%) and CD44 (99.0%) while negative for CD34 (0.21%) and CD31 (0.48%), suggesting high purity of hBMSCs. Further, these isolated hBMSCs also expressed mesenchymal and stem cell markers like nestin, β-catenin, STRO-1, α- SMA, fibronectin. The research demonstrated that fibronectin and α smooth muscle actin are equally important to maintain MSC stemness (Talele *et al.* 2015, Zeng *et al.* 2016). Further, STRO-1 is an important marker for MSC migration (LOPEZ *et al.*) and present on MCS precursor subpopulation (Dennis *et al.* 2002). Nestin and vimentin- a type III intermediate cytoskeletal protein and along with ki67-a cell proliferation marker play a crucial role in governing stemness (Kim *et al.* 2010, Méndez-Ferrer *et al.* 2010). Additionally, these cells weakly expressed some of the pluripotent stemness markers that are mainly expressed in ESCs like *C-MYC, KLF-4, OCT-4, SOX-2*, and *NANOG* indicating hBMSCs link with the embryonic stem cells (Riekstina *et al.* 2009). The multipotency of BMSCs can be exhibited by differentiating them into adipogenic, osteogenic, and chondrogenic lineage(Pittenger *et al.* 1999, Aggarwal and Pittenger 2005) which was confirmed in our study by the *in-vitro* differentiation of the purified hBMSCs into these three lineages.

Our earlier lab data showed that swertisin, one of the bioactive components of methanolic extract of plant *Enicostemma littorale*, has islet neogenic potential (Gupta *et al.* 2010) to generate ILCCs and restored normoglycemia in diabetic mice model (Dadheech *et al.* 2013). The detailed molecular mechanism of pancreatic β -cell neogenesis using swertisin was mediated by AKT-MEPK-TKK pathways which is similar to that of activin A. Activation of TGF-β signaling pathways for pancreatic islet differentiation was illustrated in 70 % partial pancreatectomised (PPx) diabetic mouse model treated with swertisin (Dadheech *et al.* 2015). The islet differentiation potential of swertisin was also evaluated in PREPS (Pancreatic resident endocrine progenitors) which were further transplanted in a diabetic mouse model (Srivastava *et al.* 2019). There are very few reports that describe islet differentiating bioactive agents such as conophylline, resveratrol, silymarins (Soto *et al.* 2014, Oh 2015, Pezzolla *et al.* 2015). Thus, we aimed at extrapolating the potentials of swertisin to differentiate hBMSCs into ILCCs with activin-A as a positive differentiation factor (Demeterco *et al.* 2000).

In order to infer that our protocol for *in vitro* islet differentiation using swertisin is successfully differentiating hBMSCs into ILCCs, we assessed the insulin transcript levels in day 10 cell clusters. However, the expected insulin levels were not achieved. A major problem in differentiated islets from stem cells is an under-expression of insulin transcript along with subnormal insulin release as compared to pancreatic islets (Zanini *et al.* 2011). One of the plausible reasons for the low insulin transcripts can be the escape of stem cells from participation in differentiation as well as cell death during differentiation. Thus, optimization of the culture conditions becomes crucial to improve the yield of ILCCs and their functional performance. Hence, the islet differentiation period was extended to 18 days along with the addition of various differentiating molecules and supplement of growth factors. This time regime was adapted from (Gabr *et al.* 2013).

DMEM high glucose and low glucose has been reported to promote islet differentiation, increase insulin expression & islet maturation respectively (Marappagounder *et al.* 2013, Czubak *et al.* 2014, Gabr *et al.* 2014, Niu *et al.* 2016). Hence, we have induced the differentiation using high glucose DMEM, and in the later stages, shifted to low glucose DMEM. After swertisin/activin A was supplemented, they could efficiently differentiate hBMSCs into ILCCs. This may indicate that swertisin /activin A could be a potent inducer for participating hBMSCs in the islet differentiation process and preventing the transformation of hBMSCs into other lineages.

hBMSCs are mesoderm origin with no direct association with pancreatic progenitors that are native in the tissue of endodermal source or development of neuro-endocrine precursor obtained from the endoderm lineage. Hence, we designed a protocol based on four-stage process (1) inducing definitive endoderm, (2) expanding pancreatic precursors, (3) generating endocrine progenitors, and (4) maturing pancreatic islets with a combination of activin A/swertisin, curcumin, genistein (BMC group) and various factors [HGF, retinoic acid, FGF, EGF, N2, B27 supplement, exendin-4, and nicotinamide] in a sequential manner for 18th day islet differentiation process. The application of activin A/swertisin, HGF, and retinoic acid-induced definitive endoderm formation (D'Amour *et al.* 2005). Retinoic acid is a key modulator of embryonic endoderm differentiation along with other key natural factors(Pan and Wright 2011) and has been used extensively *in vitro* islet differentiation to mimic the conditions during the natural pancreatic development (D'Amour *et al.* 2006, Pan and Wright 2011, Gabr *et al.* 2013). We have used retinoic acid during the initial induction stage of our protocol i.e. until day 5, in our differentiation medium along with swertisin and 1x ITS to ensure definitive endodermal differentiation from the mesodermal hBMSCs. Additionally, HGF addition in the first stage of induction culture media ensures the entry to definitive endoderm differentiation of hBMSCs (Wells and Melton 2000). Sodium butyrate was used as a proliferation-arresting compound and for chromatin remodeling to increase stem cell participation into differentiation (Simon *et al.* 1997, Goicoa *et al.* 2006). Similarly, growth factors EGF and FGF-b have been known to expand the cells and promote differentiation into a pancreatic progenitor lineage, which was added in the second stage of islet differentiation (Collombat *et al.* 2003, Gabr *et al.* 2013, Gabr *et al.* 2014). Nicotinamide is a differentiation inducer and its function is facilitated through poly (ADP-ribose) polymerase (PARP)- inhibitor. Its use in the third and fourth-stage helps to preserve islet viability and maturation (Kolb and Burkart 1999, Chen *et al.* 2004, Vaca *et al.* 2008). Exendin-4 is a glucagon-like peptide-1 mimic, which increases insulin expression and, promotes islet differentiation (Movassat *et al.* 2001, Zhou *et al.* 2002, Kassem *et al.* 2016). Activin A is playing a central role in promoting islet differentiation and maturation and increases insulin content in the differentiated cells (Demeterco *et al.* 2000). Pancreatic islets are extremely vulnerable to oxidative stress due to high endogenous production of reactive oxygen species (ROS) as opposed to a minor expression of antioxidative enzymes in β cells (Tiedge *et al.* 1997). Curcumin has been reported to show islet protective effects (Meghana *et al.* 2007), we've used it during the later stages of our protocol to ensure the survival of the islet-like cell clusters (ILCCs). In a similar context, N2 and B27 were added as supplements for

serum-free media to protect differentiated ILCCs against oxidants. Moreover less ROS observed in BMC group can be related to antioxidant and islet protective action reported earlier from our lab of methanolic extract of EL which is rich in swertisin (Srivastava *et al.* 2016). Thus, we developed an efficient stepwise protocol directed pancreatic differentiation into mature insulin-producing cells (D'Amour *et al.* 2006, Kim *et al.* 2016, Rattananinsruang *et al.* 2018). Further, we increased hBMSCs participation in differentiation by using ultralow adherence (ULA) plates, as a special hydrophilic hydrogel coating which greatly prevents cells /clusters attachment and also facilitate a good opportunity for the chemotactic movement, aggregation and 3-D cell clustering of hBMSCs (Valamehr *et al.* 2008). Very intense DTZ staining of these clusters was positive for insulin-containing vesicles which had been less observed in the cluster from the previous culture condition (10^{th} day ILCCs and 18^{th} day ILCCs in non-adherence plates). To comment on the transplantable quality of these islets like cell clusters (ILCC), we carried out the morphometric analysis and obtained 60% of the clusters to be less than 100µm in diameter which according to recent reports has been found to be an optimum size for ILCC (Ichihara *et al.* 2016).

Several pancreatic transcription factors play an important role in sustaining the phenotype of pancreatic β-cells (Bernardo *et al.* 2008). After successfully designing the four-stage protocol, we assessed the expression of all-important genes involved in islets differentiation using a custom made TLDA for ILCC derived with BMC and activin-A. In bioactive molecule cocktail derived ILCC, there was high expression of *FOXA2 & HNF1ß* (Marker for definitive endoderm), *NGN3* (Marker for pancreatic progenitors); (Lee *et al.* 2002, Wilson *et al.* 2003), *PDX1* (essential for pancreatic primordial expansion &islets development)(Gao *et al.* 2008), Nestin (Endocrine marker)(Zulewski *et al.* 2001), *MAFA & PAX4* (definitive ß cell marker)(Aramata *et al.* 2007, Lorenzo *et al.* 2017) as compared positive control. Higher gene expression of insulin was observed when compared to the positive control. Based on the expression of these markers it was confirmed that hBMSCs were successfully differentiated into functional ILCCs in both the groups. Interestingly, BMC containing swertisin demonstrated better potency as compared to activin A.

The functional benchmark for islet differentiation is the expression of mature pancreatic islet markers such as c-peptide and glucagon. Previously published reports misinterpreted the reality that the ILCCs could absorb insulin from the differentiation culture media (provided with the ITS consist of supplementary insulin). Thus, in the current study, human c-peptide was utilized

to confirm that de-novo synthesis of insulin would be produced from the ILCCs themselves and we can rule out any possibility of insulin being absorbed by cells during *in vitro* culture (Rajagopal *et al.* 2003, Hansson *et al.* 2004). The clusters were positive for these endpoint markers again indicating successful islet differentiation. The ILCCs produced on 18th day had 77 % c-peptide levels (β cell-specific marker) and 16% of glucagon producing cells (α cell-specific marker) as demonstrated by flow cytometry results, concluding that differentiated islets in the BMC group were perfectly resembling human pancreatic islets (70-80 % β-cells & 15-20 % α-cells). Very importantly, our methodology drastically enhanced the potency of hBMSCs induction to ILCCs, as compared to the earlier published investigation of only 5% to 20 % insulin-expressing cells from hBMSCs (Gabr *et al.* 2013, Jafarian *et al.* 2014, Xin *et al.* 2016).

To assess the physiological competence of bioactive molecule cocktail derived ILCC, a c-peptide release assay was performed under different glucose (2.5mM & 25mM glucose) challenge & compared with activin A derived ILCC. Human c- peptide levels were showed 1.1pg/mg protein per 60 min which was higher than our control (i.e. undifferentiated hBMSCs). Also, a group of researchers has shown the differentiation of hBMSCs to ILCCs to produce a c-peptide in response to glucose challenge (Jafarian *et al.* 2014). Recognition of c-peptide in the ILCCs confirmed that insulin release resulted from endogenous synthesis and processing. Although dynamic human c-peptide release assay showed a more sustained secretion during high glucose in ILCCs compared to hBMSCs, these results were found to be similar with some minor variation between the three BM donors.

Thus, the tested formulation of cocktail media consists of differentiating factors, several growth factors, bioactive molecules, and optimization of differentiation time was able to deliver a reproducible as well as scalable novel protocol for generating ILCCs with high c-peptide and glucagon content. However, there are multifactorial influences in the differentiation of hBMSCs into ILCCs. There are many questions left unanswered and unresolved. Further dissection of the transcriptional mechanisms controlled by various transcription factors should be studied to enhance our overall understanding of the islet differentiation from hBMSCs, which has been attempted in our next chapter.

3.6. Summary of Chpater-3

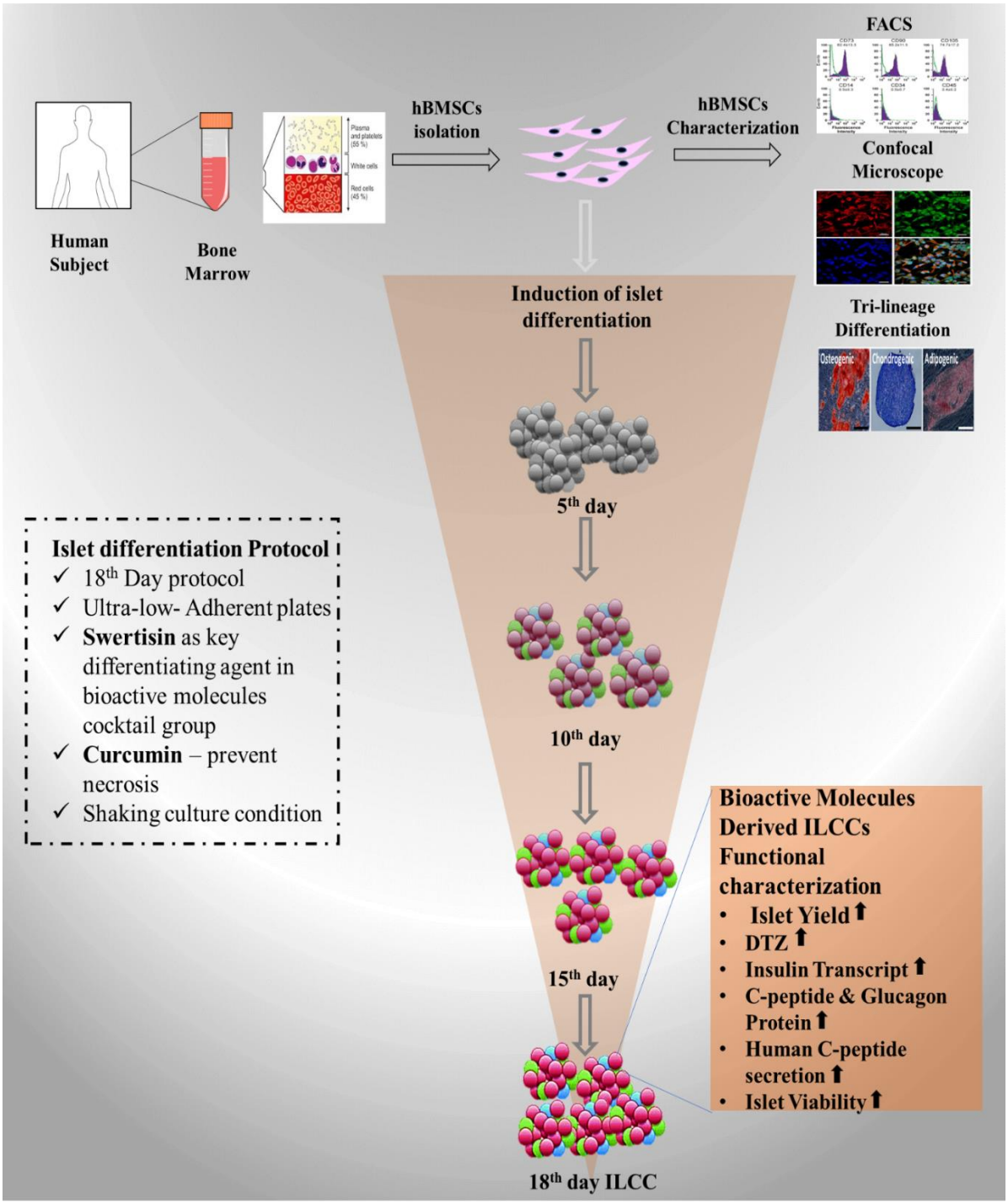

Figure 3. 24:Representative flow chart of summary of the chapter-3